Postprint of: Mawassy N., Reda H., Ganghoffer J. F., Eremeyev V. A., Lakiss H., A variational approach of homogenization of piezoelectric composites towards piezoelectric and flexoelectric effective media, International Journal of Engineering Science, Vol. 158 (2021), 103410, DOI: 10.1016/j.ijengsci.2020.103410

A variational approach of homogenization of piezoelectric composites towards piezoelectric and flexoelectric effective media

Nagham Mawassy[a], Hilal Reda[a,b], Jean-Francois Ganghoffer[c,*], Victor A. Eremeyev[d,e], Hassan Lakiss[a]

[a] *Faculty of Engineering, Section III, Lebanese University, Campus Rafic Hariri, Beirut, Lebanon*
[b] *SDM Research Group, International University of Beirut BIU, Beirut, Lebanon*
[c] *Université de Lorraine – CNRS. LEM3, UMR CNRS 7239, 7 rue Félix Savart, F-57070 Metz, France*
[d] *Gdańsk University of Technology, ul. Gabriela Narutowicza 11/12, 80-233 Gdańsk, Poland*
[e] *R. E. Alekseev Nizhny Novgorod Technical University, Minin St., 24, Nizhny Novgorod 603950, Russia*

Keywords:
Piezoelectricity
Flexoelectricity
Homogenization
Variational principles
Effective properties
Composite materials

A B S T R A C T

The effective piezoelectric properties of heterogeneous materials are evaluated in the context of periodic homogenization, whereby a variational formulation is developed, articulated with the extended Hill macrohomogeneity condition. The entire set of homogenized piezoelectric moduli is obtained as the volumetric averages of the microscopic properties of the individual constituents weighted by the displacement and polarization localization operators. This framework is extended in a second part of the paper to the computation of the flexoelectric effective properties, thereby accounting for higher gradient effects that may be induced by a strong contrast of properties of the composite constituents. The effective properties of inclusion-based composites are evaluated numerically as an illustration of the general homogenization theory and the respective effect of the volume fraction and relative tensile modulus of the reinforcement is assessed numerically.

1. Introduction

Among various electromechanical phenomena the piezoelectricity discovered by Jacques and Pierre Curie is mostly known as it found various applications in engineering, see, e.g., Maugin (1988), Eringen and Maugin (1990), Yang (2006). Nowadays there exists various natural and artificial piezoelectric materials, such as quartz, zirconate titanate (PZT), barium titanate and many others. However, piezoelectricity possesses some limitations driving the search for richer electromechanical coupling effects. Recent works from the literature are devoted to flexoelectricity, discovered relatively recently, in the 60ies, see Kogan (1964), Meyer (1969). Flexoelectricity represents the linear response of electrical polarization to the mechanical strain gradient, unlike piezoelectricity, which describes a linear coupling between the electrical polarization and mechanical strain, see Yudin and Tagantsev (2013), Zubko, Catalan and Tagantsev (2013), Nguyen et al. (2013), Wang, Gu, Zhang and Chen (2019). This higher-order electromechanical phenomenon overcomes the drawbacks of piezoelectricity. To

* Corresponding author.
E-mail addresses: nagham.mawassy@gmail.com (N. Mawassy), hilalreda@hotmail.com (H. Reda), jean-francois.ganghoffer@univ-lorraine.fr (J.-F. Ganghoffer), eremeyev.victor@gmail.com (V.A. Eremeyev), hlakiss@ul.edu.lb (H. Lakiss).

Nomenclature of the principal notations and symbols

$\mathbf{D}$	electric displacement
ϵ_0	permittivity of vacuum
$\mathbf{E}^{elec}$	electric field
$\mathbf{P}$	polarization vector
$\mathbf{u}$	displacement vector
ϕ	electric scalar potential
$\mathbf{I}$, $\mathbf{I}_2$	second order identity tensor
ρ_q^f	density of free mobile charges
Ω	volume
σ	total stress tensor
$\mathbf{f}$	body force
$\mathbf{u}$	total displacement field
ϵ	medium permittivity
t	prescribed surface traction

explain it further, while piezoelectricity gives a constant electric field, flexoelectricity leads to an electric field, which is a function of position. Flexoelectricity may exist in centrosymmetric materials, for example, in isotropic ones, whereas piezoelectricity requires non-centrosymmetric materials (Le Quang & He, 2011, Zubko, Catalan & Tagantsev, 2013). In addition to that, flexoelectricity is of high importance at nanoscales where the strain gradients increase in magnitude, while piezoelectricity vanishes (Hong, 2018). So, at small scales the flexoelectric response could be significant and even dominant. As a result, flexoelectric materials can be applied as working elements of MEMS and NEMS, such as energy harvesters, sensors, actuators, etc., see, e.g., Majdoub, Sharma and Cagin (2008), Nguyen et al. (2013), Deng, Kammoun, Erturk and Sharma (2014), Zhang, Xu, Liu and Shen (2015), Liu, Wu and Wang (2016), Wang, Gu, Zhang and Chen (2019), Ghayesh and Farajpour (2019).

Flexoelectricity must be incorporated within the framework of second gradient mechanics and accounts for a polarization gradient as done in Mindlin (1968). In such a medium, the gradient of deformation (a third order tensor) is taken into consideration in addition to the classical deformation tensor. To the contrary, the Cauchy medium considers only the first displacement gradient (Hooke's law in which the displacement is the only degree of freedom). Homogenization methods towards generalized media considering either additional degrees of freedom, like the Cosserat and Cosserat (1896), Cosserat and Cosserat (1909), Eringen, (1999) or additional higher order gradients like the second-order gradient continuum developed by Toupin (1962), Mindlin (1964) contribution aim to remedy the limitations of the classical homogenization methods. The classical homogenization techniques encounter limitations when the wavelength of the loading or deformation field becomes comparable with the typical microstructure size; it is a well-established fact in the literature (Buechner & Lakes, 2003, Park & Lakes, 1986) that the classical Cauchy theory does not allow the correct prediction of the mechanical response at sufficiently small scale levels. This requires the improvement of these theories by incorporating additional intrinsic parameters and internal length scales to correlate the microstructure with the macrostructure.

As flexoelectric response is more pronounced at small scales, flexoelectricity was taken into account for modification of theories for nanometer-sized beams and plates, see, e.g., Yue, Xu and Chen (2016), Barati (2017), Qi et al. (2018), Malikan and Eremeyev (2020) and references therein. In order to improve the piezoelectric response in the literature, various flexoelectric composite materials have been proposed, see also Liang, Zhang, Hu and Shen (2017), Shingare and Kundalwal (2019). Nowadays it is already established that considering composites made of flexoelectric materials the optimized microstructure can play a crucial role for a better performance. In particular, the effective piezoelectric response could be achieved for proper microstructure, as shown by Sharma, Maranganti and Sharma (2007) and Eremeyev, Ganghoffer, Konopińska-Zmys lowska and Uglov (2020). In order to improve the performance of composites homogenization techniques can be applied. The availability of effective properties and their dependence on microstructure enables to optimize the microstructure to increase the required response as in Casalotti, D'Annibale and Rosi (2020). Topology optimization of flexoelectric structures was discussed in Nanthakumar, Zhuang, Park and Rabczuk (2017). As flexoelectric materials can be considered as a particular class of strain gradient materials the homogenization schemes proposed for such material could be also useful, as in Rahali, Dos Reis and Ganghoffer (2017) and Abdoul-Anziz and Seppecher (2018). Unlike piezoelectric composites, see, e.g., Grekov, Kramarov and Kuprienko (1987), Sevostianov, Levin and Kachanov (2001), Chambion et al. (2011), Reda et al. (2020), up to our knowledge there exist only up to now few works on the homogenization of flexoelectric composites, see Guinovart-Sanjuán et al. (2019) for the one-dimensional case. So developing a general approach for the determination of effective properties of flexoelectric composites is of great interest.

Works devoted to the computation of the effective response of piezoelectric composites rely on multiscale methods as in Grekov, Kramarov and Kuprienko (1987), which constitute a powerful tool for the analysis of their macroscopic behavior. Such methods can handle multifield phenomena like coupled electromechanical phenomena, providing a quantitative understanding of the impact of microscale parameters on the overall multiphysical composite response. The computation

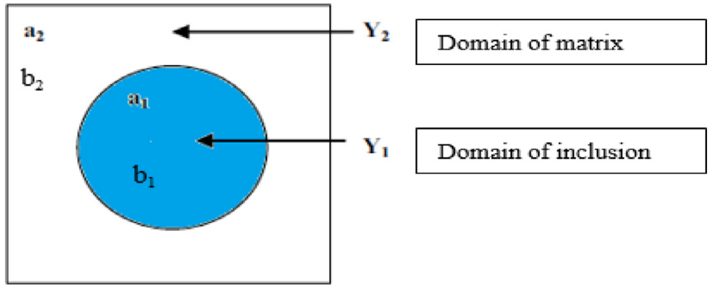

Fig. 1. Two elastic materials with rigidity and piezoelectric coefficients a_i, b_i (the index i stands for the constituent within the unit cell).

of the homogenized response of stratified piezoelectric material based on the method of oscillating functions is used by Reda et al. (2020). This method allows obtaining a homogenized response of the stratified piezoelectric structure in the form of parametric, closed form expressions that depend on the material attributes of the layers building up the repetitive unit cell. This method was inspired by the homogenization method done by Tartar (1990) and has been further extended by Cioranescu and Donato (1999). It relies on the convergence of the product of two weakly converging sequences in which a div-curl lemma was introduced for passing to this limit. The closed-form nature of the relation between the macro and micro-scales attributes can be used as a basis for tuning the macroscopic behavior by optimizing the underlying geometry and materials properties of the constituents within an identified unit cell.

The main objective of the present study is to set up a homogenization method of heterogeneous piezoelectric materials towards flexoelectric effective media, which is able to deliver the entire set of piezoelectric, and flexoelectric effective properties. The proposed method relies on the variational principle (weak formulation) articulated with Hill lemma (Hill, 1967) extended to flexoelectricity. To the knowledge of the authors, this is the first time such a general homogenization framework is proposed.

In the context of periodic homogenization, the microstructure is identified within an irreducible representative unit cell, which by periodic translation generates the entire composite domain. In the context of composite materials Fig. 1, the reinforcement has higher properties in comparison to its surrounding matrix. A state of perfect adherence at the interface between both constituents is assumed in the present work, so that both the displacement and traction are continuous across the interface between reinforcement and matrix.

The equilibrium of the macro-homogenized flexoelectric medium can be described by the two following partial differential equations:

$$\frac{\partial \mathbf{\Sigma_{ij}}}{\partial \mathbf{x_j}} - \frac{\partial^2 \mathbf{S_{ijk}}}{\partial \mathbf{x_j} \partial \mathbf{x_k}} = 0, \quad \frac{\partial \overline{\mathbf{D}}_\mathbf{i}}{\partial \mathbf{x_i}} - \frac{\partial^2 \mathbf{R_{ij}}}{\partial \mathbf{x_i} \partial \mathbf{x_j}} = 0$$

wherein $\mathbf{\Sigma_{ij}}$, $\mathbf{S_{ijk}}$, $\overline{\mathbf{D}}_\mathbf{i}$ and $\mathbf{R_{ij}}$ are respectively the stress, hyperstress, the electric displacement and the higher gradient electric displacement. Here and in the sequel, we distinguish the microscopic scale (at the scale of individual phases) within the unit cell denoted by the spatial position $\mathbf{y}$ from the macroscopic scale of the homogenized continuum (thus replacing the initially heterogeneous composite by a homogeneous substitution media with effective piezoelectric or flexoelectric properties), for which we employ the spatial position vector $\mathbf{x}$.

A few words regarding the employed notations are in order. Vectors and tensors are denoted by boldface symbols. The second and fourth order identity tensors are respectively denoted $\mathrm{I}_\mathbf{2}$ and $\mathbf{I_4}$. The gradient of a scalar field or vector with respect to the spatial position is denoted with the nabla operator and the position as a subscript. For example, $\nabla_x \mathbf{E}(\mathbf{x})$ represents the gradient of the tensor field $\mathbf{E}(\mathbf{x})$ w.r.t. to the macroscopic position, vector $\mathbf{x}$. The transpose of a tensor is written with a superscript notation, for instance $\mathbf{B^T}$. The gradient of a tensor field $\mathbf{A}(\mathbf{y})$ is denoted $\mathbf{A}(\mathbf{y}) \otimes \nabla_y$ (with $\otimes$ the tensor product) and its divergence is obtained as the trace of the gradient, $\mathbf{A}(\mathbf{y}).\nabla_y$. The symmetrized dyadic product is denoted $\otimes^s$. The dot product therein represents the inner product in the space of Cartesian tensors. The simple, double and triple contractions of tensors are written .,:, $\therefore$ respectively, so that it holds $\mathbf{A}.\mathbf{B} = A_k B_k$, $\mathbf{C}{:}\mathbf{D} = \mathrm{C}_{ij} D_{ij}$, $\mathbf{U} \therefore \mathbf{V} = \mathrm{U}_{ijk} V_{ijk}$, with $(\mathbf{A}, \mathbf{B})$, $(\mathbf{C}, \mathbf{D})$, $(\mathbf{U}, \mathbf{V})$ pairs of first order, second order and third order tensors respectively.

2. First gradient piezoelectric homogenization

In order to set the stage, we recall the strong form of the governing equations at the microlevel of the composite constituents (Moreno-Navarro et al., 2018) with a few subsequent simplifications since we primarily aim to focus on the effects of electric fields – discarding magnetic phenomena in this contribution.

The primal variables are the displacement and polarization vectors $\mathbf{u}(\mathbf{x}, t)$, $\mathbf{P}(\mathbf{x}, t)$, which enter as arguments of the electromechanical energy density. Note that polarization or electric displacement $\mathbf{D}(\mathbf{x}, t)$ can alternatively be chosen as DOF's (short cut for degrees of freedom) since they are linearly related, viz. it holds the relation

$$\mathbf{D} = \epsilon_0 \mathbf{E}^{elec} + \mathbf{P} \tag{1}$$

with ϵ_0 the permittivity of vacuum, and in which the electric field $\mathbf{E}^{elec}$ can be expressed via the electric scalar potential ϕ as follows

$$\mathbf{E}^{elec} = -\phi \otimes \nabla \tag{2}$$

The last relation automatically guarantees the satisfaction of Maxwell equation

$$\nabla x \mathbf{E}^{elec} = \mathbf{0} \tag{3}$$

The electric displacement in non-deformed media relates to the electric field and polarization as

$$\mathbf{D} = \epsilon_0 \mathbf{E}^{elec} + \mathbf{P} \equiv \epsilon_0 (\mathbf{I} + \chi_e).\mathbf{E}^{elec} = \epsilon\, \mathbf{E}^{elec} \tag{4}$$

with ϵ_0 the permittivity of vacuum, ϵ the medium permittivity, χ_e is the electric susceptibility and $\mathbf{I}$ the second order identity tensor.

Since we will focus on statics in the present paper, rate derivatives can be neglected, which entails a decoupling of the electromagnetic problem into pure electrical and pure magnetic problems:

$$\begin{aligned} &\mathbf{E}^{elec} = -\phi \otimes \nabla \\ &div\, \mathbf{D} = \rho_q^f \\ &div\, \mathbf{J} + \dot{\rho}_q^f = 0 \end{aligned} \tag{5}$$

We consider in this paper only the coupling between electric fields with mechanics and ignore magnetic fields; in this case, the local set of piezoelectric balance equations resumes to

$$\begin{aligned} &div\sigma + \mathbf{f} = \mathbf{0} \\ &\varepsilon := \frac{1}{2}\left(\mathbf{u} \otimes \nabla + \mathbf{u} \otimes \nabla^T\right) \\ &\sigma.\mathbf{n} = \mathbf{t}^d \text{ on } S_t \\ &div\mathbf{D} = \rho_q^f \\ &\mathbf{E}^{elec} = -\phi \otimes \nabla \\ &\mathbf{D}.\mathbf{n} = D^d \text{ on } S_D \\ &div\mathbf{J} = 0 \end{aligned} \tag{6}$$

Note that by virtue of the mechanical-electric analogy, the electric scalar potential is the analog of the displacement in mechanics, vector $\mathbf{u}$ in Eq. $(6)_2$, ensuring satisfaction of the kinematic compatibility condition. The force like variables $(\sigma, \mathbf{D})$ satisfy natural boundary conditions written thereabove, with $\mathbf{n}$ the unit exterior normal to the domain, and $(\mathbf{t}^d, D^d)$ are input data on the parts S_t, S_D of the domain boundary respectively. The flux like variables $(\mathbf{u}, \phi)$ satisfy natural essential boundary conditions with prescribed values on the complementary part of the domain boundary; these values are selected to be nil here and in the sequel, since they do not contribute to the effective piezoelectric moduli that will be computed.

Multiplication of the mechanical and electric balance laws, Eq. $(6)_1$ and $(6)_4$ respectively by suitable test functions, integration over the domain, integration by part with proper account of the natural boundary conditions leads to the piezoelectric strain energy density at the micro-level written in terms of the strain tensor ε and electric field $\mathbf{E}^{\mathbf{elec}}$ defining the microscopic degrees of freedom (DOF in short):

$$w_\mu(\varepsilon, \mathbf{E}^{\mathbf{elec}}) = \frac{1}{2}\left(\sigma_{\mathrm{ij}}\varepsilon_{\mathrm{ij}} + \mathrm{D_k} E_k^{elec}\right) = \frac{1}{2}\left(\mathrm{a_{kl}} E_k^{elec} E_l^{elec} + \mathrm{C_{ijkl}}\varepsilon_{\mathrm{ij}}\varepsilon_{\mathrm{kl}} + \mathrm{d_{ijk}}\varepsilon_{\mathrm{ij}} E_k^{elec} + \mathrm{d_{ijk}}\varepsilon_{\mathrm{jk}} E_i^{elec}\right) \tag{7}$$

wherein σ is the Cauchy stress, $\mathbf{D}$ the electric displacement, $\mathbf{a}$ is the tensor of dielectric (permittivity) coefficients, $\mathbf{C}$ the tensor of rigidity coefficients, and $\mathbf{d}$ the tensor of piezoelectric coefficients at the microscopic level. We have considered as a matter of simplification nil values of the traction and electric displacement in the natural boundary conditions written in Eq. (6).

The constitutive law for piezoelectric materials has the form:

$$\left| \begin{aligned} &\sigma_{\mathrm{ij}} = \mathrm{C_{ijkl}}\varepsilon_{\mathrm{kl}} + \mathrm{d_{ijk}} E_k^{elec} \\ &\mathrm{D_i} = \mathrm{a_{ij}} \mathrm{E}_j^{elec} + \mathrm{d_{ijk}}\varepsilon_{\mathrm{jk}} \end{aligned} \right. \tag{8}$$

Hill macro-homogeneity condition for piezoelectric media states that the volumetric average of the microscopic strain energy is equal to the macroscopic strain energy:

$$\left\langle w_\mu(\varepsilon, \mathbf{E}^{\mathbf{elec}})\right\rangle_Y = W_M\left(\mathbf{E}, \mathbf{E}_{\mathbf{M}}^{\mathbf{elec}}\right) = \frac{1}{2}\left(\mathbf{\Sigma} : \mathbf{E} + \mathbf{E}_{\mathbf{M}}^{\mathbf{elec}}.\overline{\mathbf{D}}\right) \tag{9}$$

wherein $\mathbf{\Sigma}$, $\mathbf{E}$, $\mathbf{E}_{\mathbf{M}}^{\mathbf{elec}}$, and $\overline{\mathbf{D}}$ are the stress, strain, electric field, and electric displacement at the mesoscopic scale respectively. The microscopic variables, namely the displacement and electric potential, are decomposed additively into a homogeneous part and a periodic fluctuating part:

$$\begin{aligned} &\mathbf{u}(\mathbf{y}) = \mathbf{u}^{\mathbf{hom}}(\mathbf{y};\mathbf{x}) + \tilde{\mathbf{u}}(\mathbf{y}) \\ &\phi(\mathbf{y}) = \phi^{\mathbf{hom}}(\mathbf{y};\mathbf{x}) + \tilde{\phi}(\mathbf{y}) \end{aligned}$$

wherein the vectors $\mathbf{u}^{hom}(\mathbf{y};\mathbf{x})$, $\phi^{hom}(\mathbf{y};\mathbf{x})$ are the homogeneous parts of the microscopic displacement and electric potential, respectively, corresponding to a heterogeneous medium that would behave exactly as a homogeneous medium. The fluctuations $\tilde{\mathbf{u}}(y)$, and $\tilde{\phi}(\mathbf{y})$ in previous decompositions account for the deviation of the postulated effective homogeneous medium from the initially heterogeneous medium. Note that these fields depend on the microscopic position and on the macroscopic position appearing as a parameter (it is indicated with a semicolon in previous expressions), as their subsequent expressions will reveal.

The vectors $\tilde{\mathbf{u}}(y)$, and $\tilde{\phi}(\mathbf{y}) \in H^1_{per}(Y)$ (the Sobolev space of Y-periodic functions) are the fluctuations that correct for the deviation of the microscopic displacement and electric potential from the displacement resulting from the homogenous strain **E(x)** and electric potential resulting from homogeneous electric field $\mathbf{E}^{\mathbf{elec}}_{\mathbf{M}}$ **(x),** respectively. Homogenization makes an upscaling of governing equations from the microscale to the macroscale, so that the resulting homogenized boundary value problem only involves macroscopic variables depending on the sole macroscopic position **x**.

An extended minimization principle of the mesoscopic energy over all periodic fluctuations holds in the absence of body forces (the subscript in $W_M(\mathbf{E},\mathbf{E}^{\mathbf{elec}}_{\mathbf{M}})$ means macroscopic),

$$W_M\left(\mathbf{E},\mathbf{E}^{\mathbf{elec}}_{\mathbf{M}}\right) = \underset{\tilde{\mathbf{u}},\tilde{\phi}\in H^1_{per}(Y)}{Min}\ \frac{1}{2}\int_Y \left\{\begin{array}{l}(\mathbf{E}+\tilde{\mathbf{u}}(\mathbf{y})\otimes\nabla_y):\mathbf{C}(\mathbf{y}):(\mathbf{E}+\tilde{\mathbf{u}}(\mathbf{y})\otimes\nabla_y)+\left(\mathbf{E}^{\mathbf{elec}}_{\mathbf{M}}-\tilde{\phi}\otimes\nabla_y\right).\mathbf{a}(\mathbf{y}).\left(\mathbf{E}^{\mathbf{elec}}_{\mathbf{M}}-\tilde{\phi}\otimes\nabla_y\right)\\ +(\mathbf{E}+\tilde{\mathbf{u}}(\mathbf{y})\otimes\nabla_y).\mathbf{d}(\mathbf{y}).\left(\mathbf{E}^{\mathbf{elec}}_{\mathbf{M}}-\tilde{\phi}\otimes\nabla_y\right)+\left(\mathbf{E}^{\mathbf{elec}}_{\mathbf{M}}-\tilde{\phi}\otimes\nabla_y\right).\mathbf{d}(\mathbf{y}).(\mathbf{E}+\tilde{\mathbf{u}}(\mathbf{y})\otimes\nabla_y)\end{array}\right\}dV_y \tag{10}$$

The stationarity condition of the previous function of the fluctuations $\tilde{\mathbf{u}}(y)$ and $\tilde{\phi}(y)$ delivers, as a necessary condition, the following boundary value problem (BVP in short) satisfied by the optimal fluctuation associated to the real displacement field (in the absence of body forces, internal force for mechanical and free charges for electric field); it describes the self-equilibrium of the unit cell:

$$\left|\begin{array}{l}-div_y\left\{\begin{array}{l}C(\mathbf{y}):(\mathbf{E}+\tilde{\mathbf{u}}\otimes\nabla_y)+\left(\mathbf{d}(\mathbf{y}).\left(\mathbf{E}^{\mathbf{elec}}_{\mathbf{M}}-\tilde{\phi}\otimes\nabla_y\right)+\left(\mathbf{E}^{\mathbf{elec}}_{\mathbf{M}}-\tilde{\phi}\otimes\nabla_y\right).\mathbf{d}(\mathbf{y})\right)+\mathbf{a}(\mathbf{y}).\left(\mathbf{E}^{\mathbf{elec}}_{\mathbf{M}}-\tilde{\phi}\otimes\nabla_y\right)\\ +(\mathbf{E}+\tilde{\mathbf{u}}\otimes\nabla_y).\mathbf{d}(\mathbf{y})+\mathbf{d}(\mathbf{y}).(\mathbf{E}+\tilde{\mathbf{u}}\otimes\nabla_y)\end{array}\right\}=\mathbf{0}\\ div_y\left\{\mathbf{a}(\mathbf{y}).\left(\mathbf{E}^{\mathbf{elec}}_{\mathbf{M}}-\tilde{\phi}\otimes\nabla_y\right)+(\mathbf{E}+\tilde{\mathbf{u}}\otimes\nabla_y).\mathbf{d}(\mathbf{y})+\mathbf{d}(\mathbf{y}).(\mathbf{E}+\tilde{\mathbf{u}}\otimes\nabla_y)\right\}=\mathbf{0}\\ \tilde{\mathbf{u}}(\mathbf{y}),\tilde{\phi}\mathrm{Y-periodic}\end{array}\right. \tag{11}$$

Since the previous BVP is linear in the loading $(\mathbf{E},\mathbf{E}^{\mathbf{elec}}_{\mathbf{M}})$ at the macroscale, the fluctuations can be written as:

$$\begin{array}{l}\tilde{\mathbf{u}}(\mathbf{y})=\mathbf{M}^{\mathbf{uE}}(\mathbf{y}):\mathbf{E}(\mathbf{x})+\mathbf{M}^{\mathbf{uP}}(\mathbf{y}).\mathbf{E}^{\mathbf{elec}}_{\mathbf{M}}(\mathbf{x})\\ \tilde{\phi}(\mathbf{y})=\mathbf{M}^{\mathbf{PE}}(\mathbf{y}):\mathbf{E}(\mathbf{x})+\mathbf{M}^{\mathbf{PP}}(\mathbf{y}).\mathbf{E}^{\mathbf{elec}}_{\mathbf{M}}(\mathbf{x})\end{array} \tag{12}$$

wherein tensors $\mathbf{M}^{\mathbf{uE}}(\mathbf{y})$, $\mathbf{M}^{PE}(\mathbf{y})$ are the displacement localizators, and $\mathbf{M}^{\mathbf{u}P}(\mathbf{y})$ and $\mathbf{M}^{PP}(\mathbf{y})$ the electric potential localizators. The localization tensors relate the microscopic DOF's to their mesoscopic counterpart. They are dependent on the microscopic position variable within the unit cell Y and are Y-periodic. Inserting these expressions into the previous BVP leads to the unit cell BVP for the first gradient piezoelectric homogenization. The previous mesoscopic energy is a function of the fluctuations, written in compact form as a Lagrangian functional of the displacement and electric potential fluctuations:

$$\begin{array}{l}L\left[\tilde{\mathbf{u}},\tilde{\phi}\right]:=\dfrac{1}{2}\displaystyle\int_Y\left\{\varepsilon:C(\mathbf{y}):\varepsilon+\mathbf{E}^{\mathbf{elec}}.\mathbf{a}.\mathbf{E}^{\mathbf{elec}}+\varepsilon.\mathbf{d}.\mathbf{E}^{\mathbf{elec}}+\mathbf{E}^{\mathbf{elec}}.\mathbf{d}.\varepsilon\right\}dV_y\\ =\dfrac{1}{2}\displaystyle\int_Y\left\{\begin{array}{l}(\mathbf{E}+\tilde{\mathbf{u}}(\mathbf{y})\otimes\nabla_y):C(\mathbf{y}):(\mathbf{E}+\tilde{\mathbf{u}}(\mathbf{y})\otimes\nabla_y)+\left(\mathbf{E}^{\mathbf{elec}}_{\mathbf{M}}-\tilde{\phi}\otimes\nabla_y\right).\mathbf{a}.\left(\mathbf{E}^{\mathbf{elec}}_{\mathbf{M}}-\tilde{\phi}\otimes\nabla_y\right)\\ +(\mathbf{E}+\tilde{\mathbf{u}}(\mathbf{y})\otimes\nabla_y).\mathbf{d}.\left(\mathbf{E}^{\mathbf{elec}}_{\mathbf{M}}-\tilde{\phi}\otimes\nabla_y\right)+\left(\mathbf{E}^{\mathbf{elec}}_{\mathbf{M}}-\tilde{\phi}\otimes\nabla_y\right).\mathbf{d}.(\mathbf{E}+\tilde{\mathbf{u}}(\mathbf{y})\otimes\nabla_y)\end{array}\right\}dV_y\end{array} \tag{13}$$

Introducing the fluctuations as a function of the localizators Eq. (12) into Eq. (13) leads to:

$$L\left[\tilde{\mathbf{u}},\tilde{\phi}\right]:=\frac{1}{2}\int_Y\left\{\begin{array}{l}\left(\mathbf{E}+\mathbf{M}^{uE}(\mathbf{y})\otimes\nabla_y:\mathbf{E}(\mathbf{x})+\mathbf{M}^{uP}(\mathbf{y})\otimes\nabla_y.\mathbf{E}^{\mathbf{elec}}_{\mathbf{M}}(\mathbf{x})\right):C(\mathbf{y})\\ :\left(\mathbf{E}+\mathbf{M}^{uE}(\mathbf{y})\otimes\nabla_y:\mathbf{E}(\mathbf{x})+\mathbf{M}^{uP}(\mathbf{y})\otimes\nabla_y.\mathbf{E}^{\mathbf{elec}}_{\mathbf{M}}(\mathbf{x})\right)\\ +\left(\mathbf{E}^{\mathbf{elec}}_{\mathbf{M}}+\mathbf{M}^{PE}(\mathbf{y}):\mathbf{E}(\mathbf{x})+\mathbf{M}^{PP}(\mathbf{y}).\mathbf{E}^{\mathbf{elec}}_{\mathbf{M}}(\mathbf{x})\right).\mathbf{a}.\left(\mathbf{E}^{\mathbf{elec}}_{\mathbf{M}}+\mathbf{M}^{PE}(\mathbf{y}):\mathbf{E}(\mathbf{x})+\mathbf{M}^{PP}(\mathbf{y}).\mathbf{E}^{\mathbf{elec}}_{\mathbf{M}}(\mathbf{x})\right)\\ +\left(\mathbf{E}+\mathbf{M}^{uE}(\mathbf{y})\otimes\nabla_y:\mathbf{E}(\mathbf{x})+\mathbf{M}^{uP}(\mathbf{y})\otimes\nabla_y.\mathbf{E}^{\mathbf{elec}}_{\mathbf{M}}(\mathbf{x})\right).\mathbf{d}.\left(\mathbf{E}^{\mathbf{elec}}_{\mathbf{M}}+\mathbf{M}^{PE}(\mathbf{y}):\mathbf{E}(\mathbf{x})+\mathbf{M}^{PP}(\mathbf{y}).\mathbf{E}^{\mathbf{elec}}_{\mathbf{M}}(\mathbf{x})\right)\\ +\left(\mathbf{E}^{\mathbf{elec}}_{\mathbf{M}}+\mathbf{M}^{PE}(\mathbf{y}):\mathbf{E}(\mathbf{x})+\mathbf{M}^{PP}(\mathbf{y}).\mathbf{E}^{\mathbf{elec}}_{\mathbf{M}}(\mathbf{x})\right).\mathbf{d}.\left(\mathbf{E}+\mathbf{M}^{uE}(\mathbf{y})\otimes\nabla_y:\mathbf{E}(\mathbf{x})+\mathbf{M}^{uP}(\mathbf{y})\otimes\nabla_y.\mathbf{E}^{\mathbf{elec}}_{\mathbf{M}}(\mathbf{x})\right)\end{array}\right\}dV_y \tag{14}$$

The effective piezoelectric constitutive law is then obtained by applying partial derivatives with respect to **E** and $\mathbf{E}^{\mathbf{elec}}_{\mathbf{M}}$, of the mesoscopic energy, which is minimized. Since the unit cell is bounded, partial derivative and integration can be switched, thus it holds using Hill extended macro-homogeneity condition the following relations:

$$\begin{array}{l}\mathbf{\Sigma}=\dfrac{\partial W_M\left(\mathbf{E},\mathbf{E}^{\mathbf{elec}}_{\mathbf{M}}\right)}{\partial\mathbf{E}}\equiv\dfrac{\partial}{\partial E}\left(\underset{\tilde{\mathbf{u}},\tilde{\phi}\in H^1_{per}(Y)}{Min}L\left[\tilde{\mathbf{u}},\tilde{\phi}\right]\right)\equiv\underset{\tilde{\mathbf{u}},\tilde{\phi}\in H^1_{per}(Y)}{Min}\dfrac{\partial L\left[\tilde{\mathbf{u}},\tilde{\phi}\right]}{\partial\mathbf{E}},\\ \overline{\mathbf{D}}=\dfrac{\partial W_M\left(\mathbf{E},\mathbf{E}^{\mathbf{elec}}_{\mathbf{M}}\right)}{\partial\mathbf{E}^{\mathbf{elec}}_{\mathbf{M}}}\equiv\dfrac{\partial}{\partial E^{elec}_M}\left(\underset{\tilde{\mathbf{u}},\tilde{\phi}\in H^1_{per}(Y)}{Min}L\left[\tilde{\mathbf{u}},\tilde{\phi}\right]\right)\equiv\underset{\tilde{\mathbf{u}},\tilde{\phi}\in H^1_{per}(Y)}{Min}\dfrac{\partial L\left[\tilde{\mathbf{u}},\tilde{\phi}\right]}{\partial\mathbf{E}^{\mathbf{elec}}_{\mathbf{M}}}\end{array} \tag{15}$$

Inserting the fluctuations as a function of the localizators Eq. (12) leads to the expressions of the effective driving forces for the piezoelectric effect:

$$\boldsymbol{\Sigma} = \frac{1}{2}\int_Y \left\{ \begin{array}{l} \left(\mathbf{E} + \mathbf{M}^{uE}\otimes\nabla_y : \mathbf{E} + \mathbf{M}^{uP}\otimes\nabla_y.\mathbf{E}_{\mathbf{M}}^{\mathbf{elec}}\right) : \mathbf{C} : \left(\mathbf{I}_4 + \mathbf{M}^{uE}\otimes\nabla_y\right) \\ +\left(\mathbf{I}_4 + \mathbf{M}^{uE}\otimes\nabla_y\right) : \mathbf{C} : \left(\mathbf{E} + \mathbf{M}^{uE}\otimes\nabla_y : \mathbf{E} + \mathbf{M}^{uP}\otimes\nabla_y.\mathbf{E}_{\mathbf{M}}^{\mathbf{elec}}\right) \\ +\left(\mathbf{E}_{\mathbf{M}}^{\mathbf{elec}} + \mathbf{M}^{PE}(\mathbf{y}) : \mathbf{E} + \mathbf{M}^{PP}.\mathbf{E}_{\mathbf{M}}^{\mathbf{elec}}\right).\mathbf{a}.\mathbf{M}^{PE} + \mathbf{M}^{PE}.\mathbf{a}.\left(\mathbf{E}_{\mathbf{M}}^{\mathbf{elec}} + \mathbf{M}^{PE} : \mathbf{E} + \mathbf{M}^{PP}.\mathbf{E}_{\mathbf{M}}^{\mathbf{elec}}\right) \\ +\left(\mathbf{I}_4 + \mathbf{M}^{uE}\otimes\nabla_y\right).\mathbf{d}.\left(\mathbf{E}_{\mathbf{M}}^{\mathbf{elec}} + \mathbf{M}^{PE} : \mathbf{E} + \mathbf{M}^{PP}.\mathbf{E}_{\mathbf{M}}^{\mathbf{elec}}\right) + \left(\mathbf{E} + \mathbf{M}^{uE}\otimes\nabla_y : \mathbf{E} + \mathbf{M}^{uP}\otimes\nabla_y.\mathbf{E}_{\mathbf{M}}^{\mathbf{elec}}\right).\mathbf{d}.\mathbf{M}^{PE} \\ +\mathbf{M}^{PE}.\mathbf{d}.\left(\mathbf{E} + \mathbf{M}^{uE}\otimes\nabla_y : \mathbf{E} + \mathbf{M}^{uP}\otimes\nabla_y.\mathbf{E}_{\mathbf{M}}^{\mathbf{elec}}\right) + \left(\mathbf{E}_{\mathbf{M}}^{\mathbf{elec}} + \mathbf{M}^{PE} : \mathbf{E} + \mathbf{M}^{PP}.\mathbf{E}_{\mathbf{M}}^{\mathbf{elec}}\right).\mathbf{d}.\left(\mathbf{I}_4 + \mathbf{M}^{uE}\otimes\nabla_y\right) \end{array} \right\} dV_y \tag{16}$$

$$\overline{\mathbf{D}} = \frac{1}{2}\int_Y \left\{ \begin{array}{l} \left(\mathbf{M}^{uP}\otimes\nabla_y\right) : \mathbf{C} : \left(\mathbf{E} + \mathbf{M}^{uE}\otimes\nabla_y : \mathbf{E} + \mathbf{M}^{uP}\otimes\nabla_y.\mathbf{E}_{\mathbf{M}}^{\mathbf{elec}}\right) \\ +\left(\mathbf{E} + \mathbf{M}^{uE}\otimes\nabla_y : \mathbf{E} + \mathbf{M}^{uP}\otimes\nabla_y.\mathbf{E}_{\mathbf{M}}^{\mathbf{elec}}\right) : \mathbf{C} : \left(\mathbf{M}^{uP}\otimes\nabla_y\right) + \left(\mathbf{I}_2 + \mathbf{M}^{PP}\right).\mathbf{a}.\left(\mathbf{E}_{\mathbf{M}}^{\mathbf{elec}} + \mathbf{M}^{PE} : \mathbf{E} + \mathbf{M}^{PP}.\mathbf{E}_{\mathbf{M}}^{\mathbf{elec}}\right) \\ +\left(\mathbf{E}_{\mathbf{M}}^{\mathbf{elec}} + \mathbf{M}^{PE} : \mathbf{E} + \mathbf{M}^{PP}.\mathbf{E}_{\mathbf{M}}^{\mathbf{elec}}\right).\mathbf{a}.\left(\mathbf{I}_2 + \mathbf{M}^{PP}\right) \\ +\left(\mathbf{M}^{uP}\otimes\nabla_y\right).\mathbf{d}.\left(\mathbf{E}_{\mathbf{M}}^{\mathbf{elec}} + \mathbf{M}^{PE} : \mathbf{E} + \mathbf{M}^{PP}.\mathbf{E}_{\mathbf{M}}^{\mathbf{elec}}\right) \\ +\left(\mathbf{E} + \mathbf{M}^{uE}\otimes\nabla_y : \mathbf{E} + \mathbf{M}^{uP}\otimes\nabla_y.\mathbf{E}_{\mathbf{M}}^{\mathbf{elec}}\right).\mathbf{d}.\left(\mathbf{I}_2 + \mathbf{M}^{PP}\right) \\ +\left(\mathbf{I}_2 + \mathbf{M}^{PP}\right).\mathbf{d}.\left(\mathbf{E} + \mathbf{M}^{uE}\otimes\nabla_y : \mathbf{E} + \mathbf{M}^{uP}\otimes\nabla_y.\mathbf{E}_{\mathbf{M}}^{\mathbf{elec}}\right) + \left(\mathbf{E}_{\mathbf{M}}^{\mathbf{elec}} + \mathbf{M}^{PE} : \mathbf{E} + \mathbf{M}^{PP}.\mathbf{E}_{\mathbf{M}}^{\mathbf{elec}}\right).\mathbf{d}.\left(\mathbf{M}^{uP}\otimes\nabla_y\right) \end{array} \right\} dV_y \tag{17}$$

In the above equations Eqs. (16) and (17), the factorization of the mesoscopic degrees of freedom ($\mathbf{E}, \mathbf{E}_{\mathbf{M}}^{\mathbf{elec}}$) leads to the expressions (A.1)–(A.2) written in **Appendix A**.

Previous expressions highlight the tensors of effective piezoelectric properties given by:

$$\left| \begin{array}{l} \boldsymbol{\Sigma} = \mathbf{C}^{\text{hom}} : \mathbf{E} + \mathbf{d}^{\mathbf{hom}}.\mathbf{E}_{\mathbf{M}}^{\mathbf{elec}} \\ \overline{\mathbf{D}} = \mathbf{d}^{\mathbf{hom}} : \mathbf{E} + \mathbf{a}^{\text{hom}}.\mathbf{E}_{\mathbf{M}}^{\mathbf{elec}} \end{array} \right. \tag{18}$$

wherein $\mathbf{C}^{\text{hom}}$, $\mathbf{d}^{\text{hom}}$, and $\mathbf{a}^{\text{hom}}$ are the effective rigidity, piezoelectric and permittivity matrices for the homogenized medium.

An alternative more compact form of the effective piezoelectric constitutive law can be formulated based on the strain localizators ($\mathbf{Z}^{\mathbf{uE}}$, $\mathbf{Z}^{\mathbf{PE}}$) and electric field localizators ($\mathbf{Z}^{\mathbf{uP}}$, $\mathbf{Z}^{\mathbf{PP}}$), elaborated in Appendix A in Eq. (A.4).

These expressions lead to the functional to be minimized, having the form of the following Lagrangian function:

$$\rightarrow L\left[\tilde{\mathbf{u}}, \tilde{\phi}\right] := \frac{1}{2}\int_Y \left\{ \begin{array}{l} \left(\mathbf{Z}^{\mathbf{uE}} : \mathbf{E} + \mathbf{Z}^{\mathbf{uP}}.\mathbf{E}_{\mathbf{M}}^{\mathbf{elec}}\right) : C(\mathbf{y}) : \left(\mathbf{Z}^{uE} : \mathbf{E} + \mathbf{Z}^{uP}.\mathbf{E}_{\mathbf{M}}^{\mathbf{elec}}\right) \\ +\left(\mathbf{Z}^{\mathbf{PE}} : \mathbf{E} + \mathbf{Z}^{\mathbf{PP}}.\mathbf{E}_{\mathbf{M}}^{\mathbf{elec}}\right).\mathbf{a}.\left(\mathbf{Z}^{\mathbf{PE}} : \mathbf{E} + \mathbf{Z}^{\mathbf{PP}}.\mathbf{E}_{\mathbf{M}}^{\mathbf{elec}}\right) \\ +\left(\mathbf{Z}^{\mathbf{uE}} : \mathbf{E} + \mathbf{Z}^{\mathbf{uP}}.\mathbf{E}_{\mathbf{M}}^{\mathbf{elec}}\right).\mathbf{d}.\left(\mathbf{Z}^{\mathbf{PE}} : \mathbf{E} + \mathbf{Z}^{\mathbf{PP}}.\mathbf{E}_{\mathbf{M}}^{\mathbf{elec}}\right) \\ +\left(\mathbf{Z}^{\mathbf{PE}} : \mathbf{E} + \mathbf{Z}^{\mathbf{PP}}.\mathbf{E}_{\mathbf{M}}^{\mathbf{elec}}\right).\mathbf{d}.\left(\mathbf{Z}^{\mathbf{uE}} : \mathbf{E} + \mathbf{Z}^{\mathbf{uP}}.\mathbf{E}_{\mathbf{M}}^{\mathbf{elec}}\right) \end{array} \right\} dV_y \tag{19}$$

By comparing Eqs. (A.5) in Appendix A and Eq. (18), the homogenized tensors $\mathbf{C}^{\text{hom}}$, $\mathbf{d}^{\text{hom}}$, and $\mathbf{a}^{\text{hom}}$ express as follows:

$$\begin{array}{l} \mathbf{C}^{\text{hom}} = \frac{1}{2}\left(\int_Y \left\{ \begin{array}{l} \left(\mathbf{Z}^{\mathbf{uE}}\right) : \mathbf{C} : \mathbf{Z}^{\mathbf{uE}} + \left(\mathbf{Z}^{\mathbf{uE}}\right)^{\mathbf{T}} : \mathbf{C} : \mathbf{Z}^{\mathbf{uE}} + \left(\mathbf{Z}^{\mathbf{PE}}\right).\mathbf{a}.\mathbf{Z}^{\mathbf{PE}} + \left(\mathbf{Z}^{\mathbf{PE}}\right)^{T}.\mathbf{a}.\mathbf{Z}^{\mathbf{PE}} \\ +\left(\mathbf{Z}^{\mathbf{uE}}\right).\mathbf{d}.\mathbf{Z}^{\mathbf{PE}} + \left(\mathbf{Z}^{\mathbf{uE}}\right)^{\mathbf{T}}.\mathbf{d}.\mathbf{Z}^{\mathbf{PE}} + \left(\mathbf{Z}^{\mathbf{PE}}\right).\mathbf{d}.\mathbf{Z}^{\mathbf{uE}} + \left(\mathbf{Z}^{\mathbf{PE}}\right)^{\mathbf{T}}.\mathbf{d}.\mathbf{Z}^{\mathbf{uE}} \end{array} \right\} dV_y \right) \\ \mathbf{d}^{\text{hom}} = \frac{1}{2}\left(\int_Y \left\{ \begin{array}{l} \left(\mathbf{Z}^{\mathbf{uE}}\right) : \mathbf{C} : \left(\mathbf{Z}^{\mathbf{uP}}\right) + \left(\mathbf{Z}^{\mathbf{uP}}\right)^{T} : \mathbf{C} : \left(\mathbf{Z}^{\mathbf{uE}}\right) + \left(\mathbf{Z}^{\mathbf{PE}}\right).\mathbf{a}.\left(\mathbf{Z}^{\mathbf{PP}}\right) + \left(\mathbf{Z}^{\mathbf{PP}}\right)^{T}.\mathbf{a}.\left(\mathbf{Z}^{\mathbf{PE}}\right) \\ +\left(\mathbf{Z}^{\mathbf{uE}}\right).\mathbf{d}.\left(\mathbf{Z}^{\mathbf{PP}}\right) + \left(\mathbf{Z}^{\mathbf{uP}}\right)^{T}.\mathbf{d}.\left(\mathbf{Z}^{\mathbf{PE}}\right) + \left(\mathbf{Z}^{\mathbf{PE}}\right).\mathbf{d}.\left(\mathbf{Z}^{\mathbf{uP}}\right) + \left(\mathbf{Z}^{\mathbf{PP}}\right)^{T}.\mathbf{d}.\left(\mathbf{Z}^{\mathbf{uE}}\right) \end{array} \right\} dV_y \right) \\ \mathbf{a}^{\text{hom}} = \frac{1}{2}\left(\int_Y \left\{ \begin{array}{l} \left(\mathbf{Z}^{\mathbf{uP}}\right) : C(\mathbf{y}) : \left(\mathbf{Z}^{uP}\right) + \left(\mathbf{Z}^{\mathbf{uP}}\right)^{T} : C(\mathbf{y}) : \left(\mathbf{Z}^{uP}\right) + \left(\mathbf{Z}^{\mathbf{PP}}\right).\mathbf{a}.\left(\mathbf{Z}^{\mathbf{PP}}\right) + \left(\mathbf{Z}^{\mathbf{PP}}\right)^{T}.\mathbf{a}.\left(\mathbf{Z}^{\mathbf{PP}}\right) \\ +\left(\mathbf{Z}^{\mathbf{uP}}\right).\mathbf{d}.\left(\mathbf{Z}^{\mathbf{PP}}\right) + \left(\mathbf{Z}^{\mathbf{uP}}\right)^{T}.\mathbf{d}.\left(\mathbf{Z}^{\mathbf{PP}}\right) + \left(\mathbf{Z}^{\mathbf{PP}}\right).\mathbf{d}.\left(\mathbf{Z}^{\mathbf{uP}}\right) + \left(\mathbf{Z}^{\mathbf{PP}}\right)^{T}.\mathbf{d}.\left(\mathbf{Z}^{\mathbf{uP}}\right) \end{array} \right\} dV_y \right) \end{array} \tag{20}$$

In the sequel, we extend the homogenization method to the consideration of higher order effects, and compute the effective flexoelectric properties.

3. Homogenization towards flexoelectric substitution media

Hill extended macro-homogeneity states that the volumetric average microscopic strain energy density is equal to the mesoscopic strain energy density:

$$\left\langle w_{\mu}\left(\varepsilon, \mathbf{E}^{\mathbf{elec}}\right)\right\rangle_Y = W_M\left(\mathbf{E}, \mathbf{E}_{\mathbf{M}}^{\mathbf{elec}}, \mathbf{K}, \mathbf{G_p}\right) = \frac{1}{2}\left(\boldsymbol{\Sigma} : \mathbf{E} + \mathbf{E}_{\mathbf{M}}^{\mathbf{elec}}.\overline{\mathbf{D}} + \mathbf{S} \therefore \mathbf{K} + \mathbf{R} : \mathbf{G}_p\right) \tag{21}$$

wherein $\mathbf{S}$ is the third-order hyperstress referring to higher gradient effects, and the second order tensor $\mathbf{R}$ is related to the higher gradient electric displacement (the second gradient electric displacement), third-order tensor $\mathbf{K}$ is the strain gradient tensor and the second-order tensor $\mathbf{G_p}$ is the electric field gradient tensor given in Eq. $(22)_4$. In view of the derivation of the effective flexoelectric properties of composites, we express the homogenous part of the microscopic displacement and electric potential as follows:

$$\begin{aligned}&\mathbf{u}^{\mathrm{hom}}=\mathbf{E}(\mathbf{x}).\mathbf{y}+\frac{1}{2}\mathbf{K}(\mathbf{x}):\mathbf{y}\otimes\mathbf{y}\\&\mathbf{K}(\mathbf{x}):=\mathbf{E}(\mathbf{x})\otimes\nabla_x\\&\phi^{\mathbf{hom}}=\mathbf{E}_{\mathbf{M}}^{\mathbf{elec}}(\mathbf{x}).\mathbf{y}+\frac{1}{2}\mathbf{G}_p(\mathbf{x}).\mathbf{y}\otimes\mathbf{y}\\&\mathbf{G}_p(\mathbf{x}):=\mathbf{E}_{\mathbf{M}}^{\mathbf{elec}}(\mathbf{x})\otimes\nabla_x\end{aligned}\tag{22}$$

The form of the displacement vector in Eq. (22) $_1$ leads to the expression of the homogeneous part of the microscopic strain as follows:

$$\varepsilon\left(\mathbf{u}^{\mathrm{hom}}\right)=\mathbf{E}(\mathbf{x})+\mathbf{K}(\mathbf{x}).\mathbf{y}\tag{23}$$

An extended minimization principle of the mesoscopic strain energy over all periodic fluctuations holds:

$$W_M\left(\mathbf{E},\mathbf{E}_{\mathbf{M}}^{\mathbf{elec}}\right)=\underset{\tilde{\mathbf{u}},\tilde{\phi}\in H^1_{per}(Y)}{Min}\ \frac{1}{2}\int_Y\left\{\begin{array}{l}(\mathbf{E}+\mathbf{K}:\mathbf{y}+\tilde{\mathbf{u}}(\mathbf{y})\otimes\nabla_y):\mathbf{C}:(\mathbf{E}+\mathbf{K}:\mathbf{y}+\tilde{\mathbf{u}}(\mathbf{y})\otimes\nabla_y)\\+\left(\mathbf{E}_{\mathbf{M}}^{\mathbf{elec}}+\mathbf{G}_p.\mathbf{y}-\tilde{\phi}\otimes\nabla_y\right).\mathbf{a}.\left(\mathbf{E}_{\mathbf{M}}^{\mathbf{elec}}+\mathbf{G}_p.\mathbf{y}-\tilde{\phi}\otimes\nabla_y\right)\\+(\mathbf{E}+\mathbf{K}:\mathbf{y}+\tilde{\mathbf{u}}(\mathbf{y})\otimes\nabla_y).\mathbf{d}.\left(\mathbf{E}_{\mathbf{M}}^{\mathbf{elec}}+\mathbf{G}_p.\mathbf{y}-\tilde{\phi}\otimes\nabla_y\right)\\+\left(\mathbf{E}_{\mathbf{M}}^{\mathbf{elec}}+\tilde{\mathbf{G}}_p.\mathbf{y}-\tilde{\phi}\otimes\nabla_y\right).\mathbf{d}.(\mathbf{E}+\mathbf{K}:\mathbf{y}+\tilde{\mathbf{u}}(\mathbf{y})\otimes\nabla_y)\end{array}\right\}dV_y\tag{24}$$

The stationarity condition of the previous functional delivers, as a necessary condition, the second order BVP to be satisfied by the optimal fluctuations associated to the real displacement field (in the absence of body forces):

$$\left|\begin{array}{l}-div_y\left\{\mathbf{C}(\mathbf{y}):(\mathbf{E}+\mathbf{K}.\mathbf{y}+\tilde{\mathbf{u}}(\mathbf{y})\otimes\nabla_y)+\mathbf{d}.\left(\mathbf{E}_{\mathbf{M}}^{\mathbf{elec}}+\mathbf{G}_p.\mathbf{y}-\tilde{\phi}\otimes\nabla_y\right)+\left(\mathbf{d}.\left(\mathbf{E}_{\mathbf{M}}^{\mathbf{elec}}+\mathbf{G}_p.\mathbf{y}-\tilde{\phi}\otimes\nabla_y\right)\right)^T\right\}=\mathbf{0},\\div_y\left\{\mathbf{a}.\left(\mathbf{E}_{\mathbf{M}}^{\mathbf{elec}}+\mathbf{G}_p.\mathbf{y}-\tilde{\phi}\otimes\nabla_y\right)+((\mathbf{E}+\mathbf{K}.\mathbf{y}+\tilde{\mathbf{u}}(\mathbf{y})\otimes\nabla_y).\mathbf{d})^T+\mathbf{d}.(\mathbf{E}+\mathbf{k}.\mathbf{y}+\tilde{\mathbf{u}}(\mathbf{y})\otimes\nabla_y)\right\}=\mathbf{0},\\\tilde{\mathbf{u}}(\mathbf{y}),\tilde{\phi}\mathrm{Y-periodic}\end{array}\right.\tag{25}$$

The fluctuations $\tilde{\mathbf{u}}(\mathbf{y})$ and $\tilde{\phi}(\mathbf{y})$ are expressed linearly versus the effective strain and electric field tensors and their gradients $\mathbf{E}(\mathbf{x}),\mathbf{E}_{\mathbf{M}}^{\mathbf{elec}}(\mathbf{x}),\mathbf{K}(\mathbf{x}),\mathbf{G}_{\mathbf{p}}(\mathbf{x})$ which constitute the loading in the BVP Eq. (25):

$$\begin{aligned}&\tilde{\mathbf{u}}(\mathbf{y})=\mathbf{M}^{uE}(\mathbf{y}):\mathbf{E}(\mathbf{x})+\mathbf{M}^{uP}(\mathbf{y}).\mathbf{E}_{\mathbf{M}}^{\mathbf{elec}}(\mathbf{x})+\mathbf{M}^{uK}(\mathbf{y})\therefore\mathbf{K}(\mathbf{x})+\mathbf{M}^{uGp}(\mathbf{y}):\mathbf{G}_p(\mathbf{x})\\&\tilde{\phi}(\mathbf{y})=\mathbf{M}^{PE}(\mathbf{y}).\mathbf{E}(\mathbf{x})+\mathbf{M}^{PP}(\mathbf{y}).\mathbf{E}_{\mathbf{M}}^{\mathbf{elec}}(\mathbf{x})+\mathbf{M}^{PK}(\mathbf{y})\therefore\mathbf{K}(\mathbf{x})+\mathbf{M}^{PGp}(\mathbf{y}):\mathbf{G}_p(\mathbf{x})\\&\mathbf{E}^{\mathbf{elec}}(\mathbf{y})=\mathbf{E}_{\mathbf{M}}^{\mathbf{elec}}+\tilde{\mathbf{E}}^{\mathbf{elec}}=\left(\mathbf{I}_2+\mathbf{M}^{PP}(\mathbf{y})\right).\mathbf{E}_{\mathbf{M}}^{\mathbf{elec}}(\mathbf{x})+\mathbf{M}^{PE}(\mathbf{y}).\mathbf{E}(\mathbf{x})+\mathbf{M}^{PK}(\mathbf{y})\therefore\mathbf{K}(\mathbf{x})+\mathbf{M}^{PGp}(\mathbf{y}):\mathbf{G}_p(\mathbf{x})\\&\Rightarrow\mathbf{E}^{\mathbf{elec}}(\mathbf{y})=\mathbf{Z}^{PP}(\mathbf{y}).\mathbf{E}_{\mathbf{M}}^{\mathbf{elec}}(\mathbf{x})+\mathbf{Z}^{PE}(\mathbf{y}).\mathbf{E}(\mathbf{x})+\mathbf{Z}^{PK}(\mathbf{y})\therefore\mathbf{K}(\mathbf{x})+\mathbf{Z}^{PGp}(\mathbf{y}):\mathbf{G}_p(\mathbf{x}),\\&\mathbf{Z}^{PK}(\mathbf{y})=\mathbf{M}^{PK}(\mathbf{y}),\\&\mathbf{Z}^{PGp}(\mathbf{y})=\mathbf{M}^{PGp}(\mathbf{y})\end{aligned}\tag{26}$$

wherein tensors $\mathbf{M^{uK}}(\mathbf{y})$ and $\mathbf{M^{PK}}(\mathbf{y})$ are the localizators for the strain gradient loading, respectively fourth- and third-order tensors. The fourth-order tensors $\mathbf{M^{uK}}(\mathbf{y}),\mathbf{M^{PK}}(\mathbf{y})$ respectively relate the fluctuating displacement to the strain gradient and the fluctuating electric potential to the strain gradient. The third-order tensors $\mathbf{M^{uGp}}(\mathbf{y})$ and $\mathbf{M^{PGp}}(\mathbf{y})$ are the localizators for the electric field gradient loading, with $\mathbf{M^{uGp}}(\mathbf{y})$ relating the fluctuating displacement to the electric field gradient. Tensor $\mathbf{M^{PGp}}(\mathbf{y})$ relates the fluctuating electric potential to the electric field gradient. Introducing the microscopic strain and electric field in terms of the strain and electric field gradients ($\mathbf{K}$, $\mathbf{G}_p$) gives the following expressions in terms of the macroscopic degrees of freedom:

$$\begin{aligned}&\mathbf{u}(\mathbf{y})\otimes\nabla_y=\left(\mathbf{u}^{\mathrm{hom}}(\mathbf{y})+\tilde{\mathbf{u}}(\mathbf{y})\right)\otimes\nabla_y\\&:=\mathbf{E}(\mathbf{x})+\mathbf{M}^{uE}(\mathbf{y})\otimes\nabla_y:\mathbf{E}(\mathbf{x})+\mathbf{K}(\mathbf{x}).\mathbf{y}+\mathbf{M}^{uK}(\mathbf{y})\otimes\nabla_y\therefore\mathbf{K}(\mathbf{x})+\mathbf{M}^{uP}(\mathbf{y})\otimes\nabla_y.\mathbf{E}_{\mathbf{M}}^{\mathbf{elec}}(\mathbf{x})\\&+\mathbf{M}^{uGp}(\mathbf{y})\otimes\nabla_y:\mathbf{G}_p(\mathbf{x})\\&\equiv\mathbf{Z}^{uE}(\mathbf{y}):\mathbf{E}(\mathbf{x})+\mathbf{Z}^{uk}(\mathbf{y})\therefore\mathbf{K}(\mathbf{x})+\mathbf{Z}^{uP}(\mathbf{y}).\mathbf{E}_{\mathbf{M}}^{\mathbf{elec}}(\mathbf{x})+\mathbf{Z}^{uG_p}(\mathbf{y}):\mathbf{G}_p(\mathbf{x}),\\&-\phi(\mathbf{y})\otimes\nabla_y=:-\left(\phi^{\mathbf{hom}}(\mathbf{y})+\tilde{\phi}(\mathbf{y})\right)\otimes\nabla_y=\mathrm{M}^{PE}(\mathbf{y}):\mathbf{E}(\mathbf{x})+\mathbf{M}^{PK}(\mathbf{y})\therefore\mathbf{K}(\mathbf{x})\\&+\mathbf{E}_{\mathbf{M}}^{\mathbf{elec}}+\mathbf{M}^{PP}(\mathbf{y}).\mathbf{E}_{\mathbf{M}}^{\mathbf{elec}}(\mathbf{x})+\mathbf{M}^{PGp}(\mathbf{y}):\mathbf{G}_p(\mathbf{x})\\&\equiv\mathbf{Z}^{PE}(\mathbf{y}):\mathbf{E}(\mathbf{x})+\mathbf{Z}^{Pk}(\mathbf{y})\therefore\mathbf{K}(\mathbf{x})+\mathbf{Z}^{,\mathbf{PP}}.\mathbf{E}_{\mathbf{M}}^{\mathbf{elec}}(\mathbf{x})+\mathbf{Z}^{,PG_p}(\mathbf{y}):\mathbf{G}_p(\mathbf{x})\end{aligned}\tag{27}$$

Using Eq. (27), the mesoscopic energy in Eq. (24) is then written in terms of the localizators as the following Lagrangian, a functional of the displacement and polarization fluctuations (see Appendix A, Eq. (A.6)).

The flexoelectric constitutive law is then obtained by taking the partial derivatives of the minimum mesoscopic energy with respect to $\mathbf{E}$ and $\mathbf{E}_{\mathbf{M}}^{\mathbf{elec}}$, $\mathbf{K}$, and $\mathbf{G}_p$ to determine the stress, electric displacement, hyperstress, and higher gradient electric displacement respectively. Since the unit cell is bounded, the partial derivative and integration can be switched (see Appendix A (A.7)–(A.11)).

Expressions (A.8)–(A.11) highlight the tensors of effective flexoelectric properties involved in the following homogenized constitutive law:

$$\left|\begin{array}{l} \boldsymbol{\Sigma} = \mathbf{C}^{\text{hom}}: \mathbf{E} + \mathbf{d}^{\mathbf{hom}}.\mathbf{E}_{\mathbf{M}}^{\mathbf{elec}} + \mathbf{B}^{\mathbf{hom}} \therefore \mathbf{K} + \mathbf{e}^{\mathbf{hom}}:\mathbf{G_P} \\ \overline{\mathbf{D}} = \mathbf{d}^{\mathbf{hom}}: \mathbf{E} + \mathbf{a}^{\mathbf{hom}}.\mathbf{E}_{\mathbf{M}}^{\mathbf{elec}} + \mathbf{F}^{\mathbf{hom}} \therefore \mathbf{K} + \mathbf{e_D}^{\mathbf{hom}}:\mathbf{G_P} \\ \mathbf{S} = \mathbf{B}^{\mathbf{hom}}: \mathbf{E} + \mathbf{F}^{\mathbf{hom}}.\mathbf{E}_{\mathbf{M}}^{\mathbf{elec}} + \mathbf{A}^{\mathbf{hom}} \therefore \mathbf{K} + \mathbf{H}^{\mathbf{hom}}:\mathbf{G_P} \\ \mathbf{R} = \mathbf{e}^{\mathbf{hom}}: \mathbf{E} + \mathbf{e_D}^{\mathbf{hom}}.\mathbf{E}_{\mathbf{M}}^{\mathbf{elec}} + \mathbf{H}^{\mathbf{hom}} \therefore \mathbf{K} + \mathbf{N}^{\mathbf{hom}}:\mathbf{G_P} \end{array}\right. \tag{28}$$

All parameters in Eq. (28) are defined for the homogenized medium at the macroscale. In details, $\mathbf{B}^{\mathbf{hom}}$ is the fifth-order coupling tensor between first gradient stress and strain gradient, $\mathbf{e}^{\mathbf{hom}}$ the fourth-order coupling tensor between the first gradient stress and second gradient electrical field. $\mathbf{F}^{\mathbf{hom}}$ the fourth-order coupling tensor between first gradient electrical displacement and second gradient strain. $\mathbf{e_D}^{\mathbf{hom}}$ is the third-order coupling tensor between the first gradient electrical displacement and the second gradient electrical field. $\mathbf{A}^{\mathbf{hom}}$ is the sixth-order second gradient tensor. $\mathbf{H}^{\mathbf{hom}}$ is the fifth-order coupling tensor between hyperstress and the second gradient electrical field, and $\mathbf{N}^{\mathbf{hom}}$ is the fourth-order coupling tensor between second the gradient electrical displacement and the second gradient electrical field.

As done in Section 2, a comparison between Eqs. (A.8), (A.9), (A.10), and (A.11) allows the determination of the tensors of homogenized properties $\mathbf{C}^{\text{hom}}$, $\mathbf{d}^{\mathbf{hom}}$, $\mathbf{B}^{\mathbf{hom}}$, $\mathbf{e}^{\mathbf{hom}}$, $\mathbf{a}^{\mathbf{hom}}$, $\mathbf{F}^{\mathbf{hom}}$, $\mathbf{e_D}^{\mathbf{hom}}$, $\mathbf{A}^{\mathbf{hom}}$, $\mathbf{H}^{\mathbf{hom}}$, $\mathbf{N}^{\mathbf{hom}}$ as corresponding integrals of microscopic quantities over the unit cell; these tensors receive however complicated expressions that will not be explicitly written.

4. Algorithm for the evaluation of the homogenized piezoelectric and flexoelectric moduli

Starting from the theoretical framework mentioned in the previous section, we propose a numerical algorithm to determine the effective tensors of the homogenized constitutive law for the second gradient flexoelectric medium. The microscopic stress σ and electric displacement $\mathbf{D}$ are given by the following constitutive relations:

$$\begin{array}{l} \sigma(y) = \mathbf{C}(y): \varepsilon(y) + \mathbf{d}(y).E^{elec}(y) \\ \mathbf{D}(y) = \mathbf{d}(y): \varepsilon(y) + \mathbf{a}(y).E^{elec}(y) \end{array} \tag{29}$$

where $\mathbf{C(y)}$ is the (microscopic) rigidity matrix, $\mathbf{d(y)}$ the (microscopic) coupling matrix between the elastic and electric fields**,** $\mathbf{a(y)}$ the (microscopic) permittivity matrix, $\varepsilon(y)$ and E^{elec} **(y)** are the (microscopic) deformation and electric fields respectively.

The microscopic deformation and electric field tensors can be decomposed into their homogeneous and fluctuating parts by introducing the macroscopic deformation, the gradient of deformation, the macroscopic electric field, and the gradient of electric field, tensors $\mathbf{E}, \mathbf{K}, \mathbf{E}_{\mathbf{M}}^{\mathbf{elec}}, \mathbf{G_P}$, respectively, as follows:

$$\begin{array}{rl} \varepsilon(\mathbf{y}) = & \varepsilon^{\text{hom}}(\mathbf{x}) + \tilde{\varepsilon}(\mathbf{y}), \\ \varepsilon^{\text{hom}}(\mathbf{x}) := & \mathbf{u}^{\text{hom}}(\mathbf{y}) \otimes^S \nabla_y = \mathbf{E} + \mathbf{K}.\mathbf{y} \end{array} \tag{30}$$

$$\begin{array}{l} \boldsymbol{\varepsilon}(\mathbf{y}) = \boldsymbol{\varepsilon}^{\text{hom}}(\mathbf{x}) + \tilde{\boldsymbol{\varepsilon}}(\mathbf{y}), \\ \boldsymbol{\varepsilon}^{\text{hom}}(\mathbf{x}) := \mathbf{u}^{\text{hom}}(\mathbf{y}) \otimes^{S} \nabla_{y} = \mathbf{E} + \mathbf{K}.\mathbf{y} \end{array}$$

$$\begin{array}{l} \mathbf{E}^{\mathbf{elec}}(\mathbf{y}) = -\phi \otimes \nabla = \mathbf{E}_{\mathbf{M}}^{\mathbf{hom\ elec}}(\mathrm{x}) + \tilde{\mathbf{E}}^{\mathbf{elec}}(\mathbf{y}), \\ \mathbf{E}_{\mathbf{M}}^{\mathbf{hom\ elec}}(\mathrm{x}) := \mathbf{E}_{\mathbf{M}}^{\mathbf{elec}} + \mathbf{G}_{\mathrm{P}}.\mathbf{y} \end{array} \tag{31}$$

wherein $\tilde{\varepsilon}(\mathbf{y})$ represents the fluctuating part of the microscopic strain, namely the symmetrical part of the microscopic gradient of the (microscopic) fluctuation $\tilde{\mathbf{u}}(\mathbf{y})$ and ϕ is the (scalar) electric potential.

At the micro-scale, the materials are considered as linear elastic and isotropic (knowing that they should be transversely isotropic but since the direction of transverse isotropy is orthogonal to our plane of study, we have isotropy within the 2D section considered in this example). In this context, the elastic stress at a point is related to the deformation at the same point by the two Lame coefficients (λ, η), with $\lambda = \frac{E\nu}{(1+\nu)(1-2\nu)}$ the first Lame's first parameter and $\eta = \frac{E}{2(1+\nu)}$ the second Lame parameter, expressed versus Young's modulus E and Poisson's ratio ν. Taking into consideration Eqs. (29), (30), (31), the microscopic stress and electrical displacement can be written in matrix format as:

$$\begin{pmatrix}\sigma_{11}\\ \sigma_{22}\\ \sigma_{12}\\ D_1\\ D_2\end{pmatrix}=\begin{pmatrix}\lambda+2\eta & \lambda & 0 & d_{11} & d_{21}\\ \lambda & \lambda+2\eta & 0 & d_{12} & d_{22}\\ 0 & 0 & 2\eta & d_{13} & d_{23}\\ d_{11} & d_{12} & d_{13} & a_{11} & 0\\ d_{21} & d_{22} & d_{23} & 0 & a_{22}\end{pmatrix}\begin{pmatrix}\tilde{\varepsilon}_{11}+E_{11}+K_{111}.y_1+K_{112}.y_2\\ \tilde{\varepsilon}_{22}+E_{22}+K_{221}.y_1+K_{222}.y_2\\ \tilde{\varepsilon}_{12}+E_{12}+K_{121}.y_1+K_{122}.y_2\\ \tilde{E}_1^{elec}+E_{M\ 1}^{elec}+G_{P11}.y_1+G_{P12}.y_2\\ \tilde{E}_2^{elec}+E_{M\ 2}^{elec}+G_{P12}.y_1+G_{P22}.y_2\end{pmatrix} \tag{32}$$

where (y_1, y_2) is the microscopic position vector in 2D situations to which we restrict the analysis here and in the sequel. The macroscopic deformation $\mathbf{E}$, the macroscopic gradient of deformation $\mathbf{K}$, the macroscopic electric field $\mathbf{E_M^{elec}}$, and the macroscopic gradient of electric field $\mathbf{G}_P$ are considered as kinematic controls applied to the unit cell Y.

The objective is to find the total displacement $\mathbf{u}$ of the unit cell BVP such that the microscopic displacement $\mathbf{u}$ and the microscopic electric field $\mathbf{E_M^{elec}}$ satisfy the following set of governing equations:

$$\left|\begin{array}{l} div_y\sigma(\mathbf{y})=\mathbf{0}\quad in\ Y\\ div_y\mathbf{D}(\mathbf{y})=0\\ \sigma(\mathbf{y})=\mathbf{C}(y):\varepsilon(\mathbf{y})+\mathbf{d}^T(\mathbf{y}).\mathbf{E^{elec}}(\mathbf{y})\ \ in\ Y\\ \mathbf{D}(\mathbf{y})=\mathbf{a}(\mathbf{y}).\mathbf{E^{elec}}(\mathbf{y})+\varepsilon(y):\mathbf{d}(\mathbf{y})\\ \varepsilon(y)=\mathbf{E}+\mathbf{K}.\mathbf{y}+\tilde{\varepsilon}(\mathbf{y})\\ \tilde{\varepsilon}(\mathbf{y}):=\tilde{\mathbf{u}}(\mathbf{y})\otimes^S\nabla_y\\ \mathbf{E^{elec}}=\mathbf{E_M^{elec}}+\mathbf{G_P}.\mathbf{y}+\tilde{\mathbf{E}}^{\mathbf{elec}}\end{array}\right. \tag{33}$$

A weak formulation of Eq. (33) is introduced to get the following formal homogenized problem, considering the decomposition of the total microscopic deformation and electric fields, $\varepsilon=\mathbf{E}+\mathbf{K}.\mathbf{y}+\tilde{\varepsilon}$, $\mathbf{E^{elec}}=\mathbf{E_M^{elec}}+\mathbf{G_P}.\mathbf{y}+\tilde{\mathbf{E}}^{\mathbf{elec}}$:

$$\forall\mathbf{v}\in H_1(Y),\ \int_Y\left(C(\mathbf{y}):\varepsilon(\mathbf{u})+\mathbf{d}^T(\mathbf{y}).\mathbf{E^{elec}}(\mathbf{y})\right):\varepsilon_a(\mathbf{v})dV_y-\int_Y\left(\mathbf{a}(\mathbf{y}).\mathbf{E^{elec}}(\phi)+\varepsilon(y):\mathbf{d}(\mathbf{y})\right).\mathbf{E^{elec}}_a(\psi)dV_y=0 \tag{34}$$

$$\begin{aligned}&\forall\mathbf{v}\in H_1(Y),\\ &\int_Y\left(C(\mathbf{y}):(\tilde{\varepsilon}+\mathbf{E}+\mathbf{K}.\mathbf{y})+\mathbf{d}^T(\mathbf{y}).\left(\mathbf{E_M^{elec}}+\mathbf{G_P}.\mathbf{y}+\tilde{\mathbf{E}}^{\mathbf{elec}}\right)\right):\varepsilon_a(\mathbf{v})dV_y\\ &-\int_Y\left(\mathbf{a}(\mathbf{y}).\left(\mathbf{E_M^{elec}}+\mathbf{G_P}.\mathbf{y}+\tilde{\mathbf{E}}^{\mathbf{elec}}\right)+(\tilde{\varepsilon}+\mathbf{E}+\mathbf{K}.\mathbf{y}):\mathbf{d}(\mathbf{y})\right).\mathbf{E^{elec}}_a(\psi)dV_y\ =0\end{aligned} \tag{35}$$

where $\mathbf{v}$ and ψ are the test functions. By solving this variational formulation, the periodic fluctuating displacement $\tilde{\mathbf{u}}$ and fluctuating electric potential $\tilde{\phi}$ satisfying Eq. (34) are obtained. This problem is solved using FreeFem++ open source finite element software as well as for the subsequent determination of the first gradient, second gradient, and the piezoelectric and flexoelectric moduli in Eq. (28).

4.1. Determination of the homogenized first and second gradient moduli

The goal in this section is to determine the first gradient moduli $\mathbf{C}^{\text{hom}}$ (rigidity matrix), second gradient modulus $\mathbf{A}^{\text{hom}}$ and the coupling tensor $\mathbf{B}^{\text{hom}}$ between first and second gradient terms. The coupling matrix between the electrical displacement and second gradient strain $\mathbf{F}^{\text{hom}}$ will also be determined. Applying the mesoscopic deformation $\mathbf{E}$ as the sole kinematic boundary condition over the unit cell leads to the first effective rigidity matrix $\mathbf{C}^{\text{hom}}$, while applying the gradient of deformation $\mathbf{K}$ alone as a kinematic boundary condition over the unit cell entails the evaluation of $\mathbf{B}^{\text{hom}}$ (the coupling matrix between the first gradient stress and second gradient strain) and $\mathbf{F}^{\text{hom}}$. Using the expression of the hyperstress, determined by applying tensor $\mathbf{K}$ only, we finally obtain the second gradient rigidity matrix $\mathbf{A}^{\text{hom}}$. This procedure is condensed in algorithmic format in Fig. 2.

The first gradient homogenization tensor $\mathbf{C}^{\text{hom}}$, and the coupling moduli $\mathbf{B}^{\text{hom}}$, and $\mathbf{F}^{\text{hom}}$ are written in the form:

$$\mathbf{C}^{\text{hom}}:\mathbf{E}=\frac{1}{|\mathrm{Y}|}\int\mathbf{C}(\mathbf{y}):\varepsilon(\mathbf{u})dV_y \tag{36}$$

$$\mathbf{B}^{\text{hom}}\therefore\mathbf{K}=\frac{1}{|\mathrm{Y}|}\int\mathbf{C}(\mathbf{y}):\varepsilon(\mathbf{u})dV_y \tag{37}$$

$$\mathbf{F}^{\text{hom}}\therefore\mathbf{K}=\frac{1}{|\mathrm{Y}|}\int\mathbf{D}dV_y \tag{38}$$

where $|Y|$ is the volume (the area in 2D) of the unit cell.

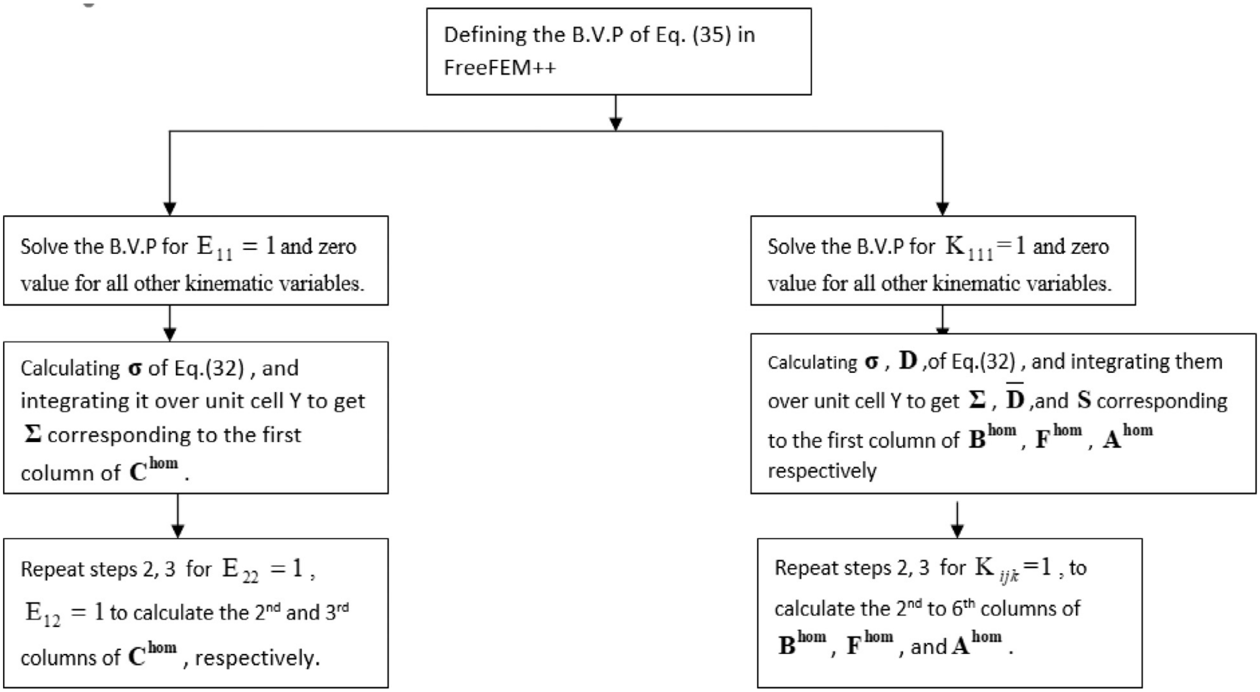

Fig. 2. Schematic diagram for the computation of the effective moduli C^{hom}, B^{hom}, F^{hom}, A^{hom}.

The average macroscopic hyperstress is written according to the Hill Lemma, as follows:

$$\mathbf{S_{ijk}} = \frac{\partial W_M}{\partial \mathbf{K_{ijk}}} = \frac{\partial}{\partial \mathbf{K_{ijk}}} \langle w_\mu(\varepsilon) \rangle_Y = \left\langle \frac{\partial w_\mu(\varepsilon)}{\partial K_{ijk}} \right\rangle_Y = \left\langle \frac{\partial w_\mu(\varepsilon)}{\partial \varepsilon_{ij}} \frac{\partial \varepsilon_{ij}}{\partial K_{ijk}} \right\rangle_Y = \left\langle \sigma_{\mathbf{ij}} \frac{\partial \varepsilon_{\mathbf{ij}}}{\partial \mathbf{K_{ijk}}} \right\rangle_Y \tag{39}$$

in which the bracket denotes the volume integration over the unit cell, normalized by the unit cell volume. The microscopic deformation field evaluated from the perturbation displacement (using the boundary value problem in Eq. (35)) and used in Eq. (39) is:

$$\begin{cases} \varepsilon_{11} = \tilde{\varepsilon}_{11} + E_{11} + K_{111}y_1 + K_{112}y_2 \equiv \frac{\partial u_1(y_1,y_2)}{\partial y_1}, \\ \varepsilon_{22} = \tilde{\varepsilon}_{22} + E_{22} + K_{221}y_1 + K_{222}y_2 \equiv \frac{\partial u_2(y_1,y_2)}{\partial y_2}, \\ \varepsilon_{12} = \tilde{\varepsilon}_{12} + E_{21} + \frac{1}{2}(K_{121} + K_{211})y_1 + \frac{1}{2}(K_{122} + K_{212})y_2 \equiv \frac{1}{2}\left(\frac{\partial u_1(y_1,y_2)}{\partial y_2} + \frac{\partial u_2(y_1,y_2)}{\partial y_1}\right) \end{cases} \tag{40}$$

The tensor $\mathbf{A}^{hom}$ is equal to the hyperstress in this case:

$$\mathbf{A}^{hom} \therefore \mathbf{K} = \frac{1}{|Y|} \int \left(\sigma_{\mathbf{ij}} \frac{\partial \varepsilon_{\mathbf{ij}}}{\partial \mathbf{K_{ijk}}} \right) dV_y \tag{41}$$

4.2. Determination of the homogenized piezoelectric and flexoelectric moduli

In this section, the tensors of effective moduli related to piezoelectricity $\mathbf{d}^{hom}$, $\mathbf{a}^{hom}$, and flexoelectricity $\mathbf{H}^{\mathbf{hom}}$, $\mathbf{e_D}^{\mathbf{hom}}$ $\mathbf{e}^{\mathbf{hom}}$, and $\mathbf{N}^{\mathbf{hom}}$ are determined. By selecting the mesoscopic deformation $\mathbf{E} = \mathbf{1}$ and applying only vector $\mathbf{P}$ as a kinematic boundary condition over the RVE, the piezoelectric matrix $\mathbf{d}^{hom}$ and permittivity matrix $\mathbf{a}^{hom}$ are obtained, while, by selecting $\mathbf{K} = \mathbf{1}$ and applying, only, $\mathbf{G_P}$ as a kinematic boundary condition over the RVE, the matrices $\mathbf{e}^{hom}$, $\mathbf{e_D}^{hom}$, $\mathbf{H}^{hom}$ and $\mathbf{N}^{\mathbf{hom}}$ are determined. This procedure is written in algorithmic format in Fig. 3.

The tensors $\mathbf{d}^{hom}$, $\mathbf{a}^{hom}$, $\mathbf{e}^{hom}$ and $\mathbf{e_D}^{hom}$ are obtained from the relations:

$$\mathbf{d}^{hom}.\mathbf{E_M^{elec}} = \frac{1}{|Y|} \int \mathbf{C}(\mathbf{y}) : \varepsilon(u) dV_y - \mathbf{C}^{hom} : \mathbf{E} \tag{42}$$

$$\mathbf{a}^{hom}.\mathbf{E_M^{elec}} = \frac{1}{|Y|} \int \mathbf{D} dV_y - \mathbf{d}^{hom} : \mathbf{E} \tag{43}$$

$$\mathbf{e}^{hom} : \mathbf{G_P} = \frac{1}{|Y|} \int \mathbf{C}(\mathbf{y}) : \varepsilon(\mathbf{y}) dV_y - \mathbf{B}^{hom} : \mathbf{K} \tag{44}$$

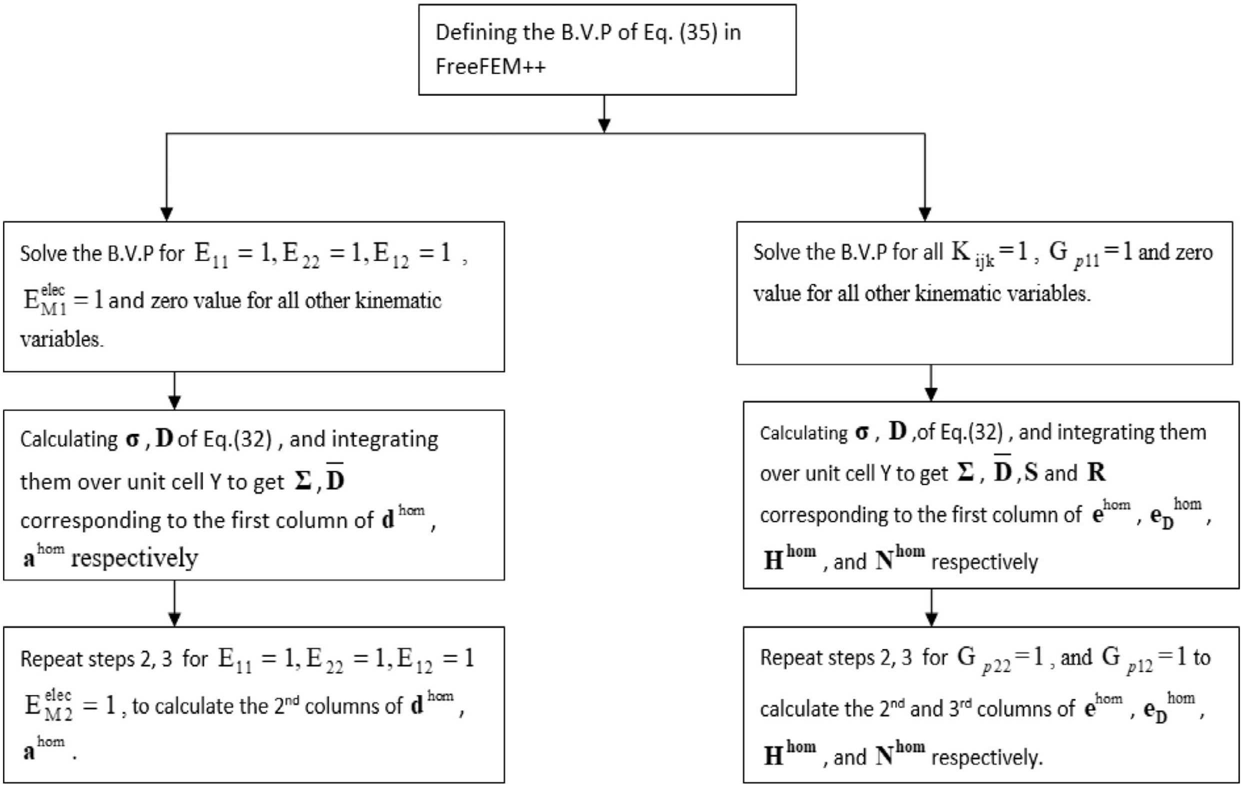

Fig. 3. Schematic diagram for computing the effective d^{hom}, a^{hom}, e^{hom}, eD^{hom}, H^{hom}, N^{hom} matrices.

$$\mathbf{e_D}^{hom} : \mathbf{G_P} = \frac{1}{|Y|}\int \mathbf{D} dV_y - \mathbf{F}^{hom} \therefore \mathbf{K} \tag{45}$$

The macroscopic second gradient electric displacement $\mathbf{R}$ is written according to Hill Lemma as follows:

$$R_{ij} = \left\langle D_i \frac{\partial E_i^{elec}}{\partial G_{ij}} \right\rangle_Y \tag{46}$$

wherein the microscopic electric field is determined from the perturbation electric potential (evaluated by solving the B.V.P Eq. (35)), and can be written according to Eq. (33) $_7$ as:

$$\begin{cases} E_1^{elec} = \tilde{E}_1^{elec} + E_{M1}^{elec} + G_{P11}y_1 + G_{P12}y_2 \\ E_2^{elec} = \tilde{E}_2^{elec} + E_{M2}^{elec} + G_{P12}y_1 + G_{P22}y_2 \end{cases} \tag{47}$$

The tensors $\mathbf{H^{hom}}$ and $\mathbf{N^{hom}}$ are determined from the relations:

$$\mathbf{H^{hom}} : \mathbf{G_P} = \frac{1}{|Y|}\int \left(\sigma_{\mathbf{ij}} \frac{\partial \varepsilon_{\mathbf{ij}}}{\partial \mathbf{K_{ijk}}}\right) dV_y - \mathbf{A^{hom}} \therefore \mathbf{K} \tag{48}$$

$$\mathbf{N^{hom}} : \mathbf{G_P} = \frac{1}{|Y|}\int \left(D_i \frac{\partial E_i^{elec}}{\partial G_{ij}}\right) dV_y - \mathbf{H^{hom}} \therefore \mathbf{K} \tag{49}$$

5. Response of 2D flexoelectric composite materials in a reduced 1D space

In the current section, we analyze the effect of the nature of effective continuum, either piezoelectric or flexoelectric on the static and piezoelectric properties of materials in a reduced 1D space. To that scope, we consider a straight beam of length L (L=1m) incorporating a 2D reinforced composite material as a unit cell, as illustrated in Fig. 1. The beam is held fixed at its left end and loaded with a constant stress Σ_0=100MP at its right end (Fig. 4). The materials considered for the two-unit cell constituents are Lithium Niobate $LiNbO_3$ for the inclusion, and Polyvinylidene Fluoride PVDF for the matrix as in Chambion et al.(2011). The properties of these piezoelectric materials are listed in Table 1. (Considering the isotropic plane as the plane of our study in 2D knowing that, in 3D, the materials are transversely isotropic).

We aim to replace the initial heterogeneous, micro-structured beam with a homogeneous beam with effective flexoelectric properties. In order to study the behavior of the flexoelectric (solving for the deformation and electric fields) effective

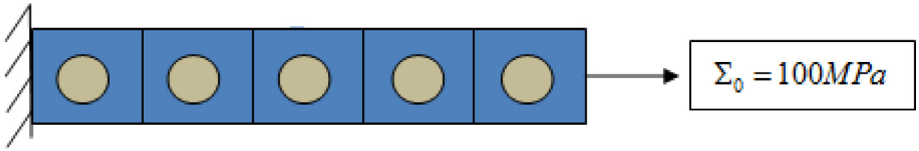

Fig. 4. 1D flexoelectric beam incorporating many repetitive unit cells along its length.

Table 1
Mechanical and electrical properties of the two piezoelectric materials within the unit cell of the composite material.

	LiNbO3 inclusion	PVDF matrix
Elastic modulus (MPa)	170000	2450
Poisson's ratio	0.25	0.34
d_{11} (pC/N)	20	0
d_{12} (pC/N)	20	0
d_{13} (pC/N)	0	0
d_{21} (pC/N)	-0.9	20
d_{22} (pC/N)	-0.9	3
d_{23} (pC/N)	6	-46
a_{11} (pF/m)	384.975	79.65
a_{22} (pF/m)	265.5	79.65

beam we write the homogenized constitutive law in the present 1D context as follows:

$$\begin{aligned}
\Sigma_{11} &= C^{\text{hom}}{}_{11}E_{11} + d^{\text{hom}}{}_{11}E^{elec}_{M}{}_{1} + B^{\text{hom}}{}_{11}K_{111} + e^{\text{hom}}{}_{11}G_{P11} \\
\overline{D}_{11} &= d^{\text{hom}}{}_{11}E_{11} + a^{\text{hom}}{}_{11}E^{elec}_{M}{}_{1} + F^{\text{hom}}{}_{11}K_{111} + e_D{}^{\text{hom}}{}_{11}G_{P11} \\
S_{111} &= B^{\text{hom}}{}_{11}E_{11} + F^{\text{hom}}{}_{11}E^{elec}_{M}{}_{1} + A^{\text{hom}}{}_{11}K_{111} + H^{\text{hom}}{}_{11}G_{P11} \\
R_{11} &= e^{\text{hom}}{}_{11}E_{11} + e_D{}^{\text{hom}}{}_{11}E^{elec}_{M}{}_{1} + H^{\text{hom}}{}_{11}K_{111} + N^{\text{hom}}{}_{11}G_{P11}
\end{aligned} \tag{50}$$

The specific cases of rigid conductors and pure strain gradient mechanics are next considered with a special emphasis.

5.1. Case of rigid conductors

The strain energy for a rigid body is identified to the volumetric average of the microscopic strain energy density and is written as a bilinear form of the electrical measures.

$$\begin{aligned}
&W_M\left(\mathbf{E^{elec}_M}, \mathbf{G_P}\right) = \frac{1}{2}\mathbf{E^{elec}_M}.a^{\text{hom}}.\mathbf{E^{elec}_M} + \frac{1}{2}\mathbf{G_P} : N^{\text{hom}} : \mathbf{G_P} + \mathbf{E^{elec}_M}.\left(e_D{}^{\text{hom}} + e_D{}^{\text{hom},T}\right) : \mathbf{G_P} \\
&= \left\langle w_\mu\left(\mathbf{E}^{elec}\right)\right\rangle_Y = \left\langle \frac{1}{2}\mathbf{E}^{elec}(\mathbf{y}).a(\mathbf{y}).\mathbf{E}^{elec}(\mathbf{y})\right\rangle_Y
\end{aligned} \tag{51}$$

Neglecting mechanical deformations leads to the following 1D higher gradient constitutive law (a specific case of previous constitutive law, Eq. (50)):

$$\begin{aligned}
\Sigma_{11} &= d^{\text{hom}}{}_{11}E^{elec}_{M}{}_{1} + e^{\text{hom}}{}_{11}G_{P11} \\
\overline{D}_{11} &= a^{\text{hom}}{}_{11}E^{elec}_{M}{}_{1} + e_{D_{11}}^{\text{hom}}G_{P11} \\
R_{11} &= e_{D_{11}}^{\text{hom}}E^{elec}_{M}{}_{1} + N^{\text{hom}}{}_{11}G_{P11} \\
S_{111} &= F^{\text{hom}}{}_{11}E^{elec}_{M}{}_{1} + H^{\text{hom}}{}_{11}G_{P11}
\end{aligned} \tag{52}$$

Considering a piezoelectric medium without higher gradient parameters, the consititive law is written in terms of the piezoelectric matrix which contains only $d^{\text{hom}}{}_{11}$Eq. (53) (in the case of rigid conductor the deformtion is nil). The electric field shows a constant value for all positions (Fig. 3).

$$\Sigma_{11} = \Sigma_0 = d^{\text{hom}}{}_{11}E^{elec}_{M}{}_{1} \rightarrow E^{elec}_{M}{}_{1} = \frac{\Sigma_0}{d^{\text{hom}}{}_{11}} \tag{53}$$

In contrast to this, when the higher gradient term $e^{\text{hom}}{}_{11}$ is considered, an exponential decrease of the electric field with position is observed, as described in Eq. (54), with the effective electric field plotted versus spatial position along the beam in Fig. 5. The spatial distribution of the electric field highlights a boundary layer closed to the left edge of the beam for an adopted left edge boundary condition of nil polarization incompatible with the first gradient solution:

$$\Sigma_{11} = \Sigma_0 = d^{\text{hom}}{}_{11}E^{elec}_{M}{}_{1} + e^{\text{hom}}{}_{11}G_{11} \rightarrow E^{elec}_{M}{}_{1} = \frac{\Sigma_0}{d^{\text{hom}}{}_{11}}\left(1 - \exp^{-\frac{d^{\text{hom}}{}_{11}}{e^{\text{hom}}{}_{11}}x}\right) \tag{54}$$

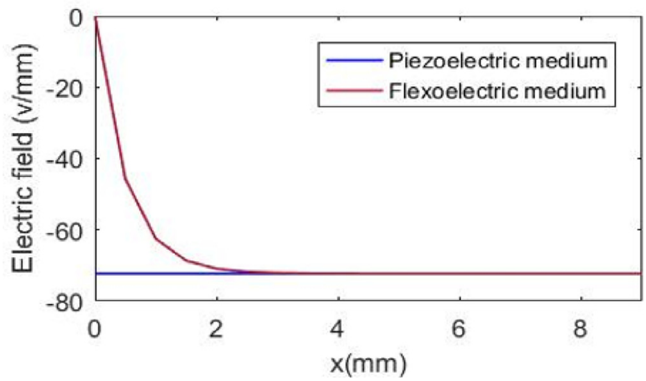

Fig. 5. Electric field with and without flexoelectric term under a constant applied stress Σ_0.

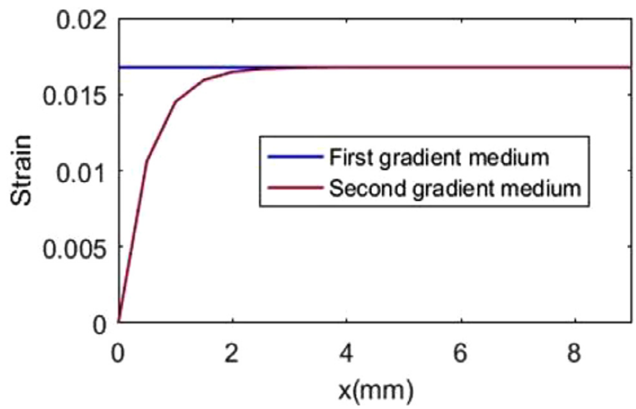

Fig. 6. Deformation with and without second gradient terms.

The flexoelectric effect is clearly apparent in Fig. 4, which shows a boundary layer close to the left side of the macro beam.

5.2. Specific case of strain gradient mechanics

The strain energy of the effective strain gradient continuum is written as the following bilinear form of the kinematic measures and is further identified to the volumetric average of the microscopic strain energy density

$$\begin{aligned} W_M(\mathbf{E},\mathbf{K}) &= \tfrac{1}{2}\mathbf{E}:C^{\text{hom}}:\mathbf{E}+\tfrac{1}{2}\mathbf{K}\therefore A^{\text{hom}}:\mathbf{K}+\mathbf{E}:\left(B^{\text{hom}}+B^{\text{hom},T}\right):\mathbf{K} \\ &= \langle w_\mu(\varepsilon)\rangle_Y = \left\langle \tfrac{1}{2}\varepsilon(\mathbf{y}):C(\mathbf{y}):\varepsilon(\mathbf{y})\right\rangle_Y \end{aligned} \tag{55}$$

Neglecting the electrical field, and referring to Eq. (50) leads to the following 1D constitutive law in a higher gradient formulation:

$$\begin{aligned} \Sigma_{11} &= C^{\text{hom}}{}_{11}E_{11}+B^{\text{hom}}{}_{11}K_{111} \\ \overline{D}_{11} &= d^{\text{hom}}{}_{11}E_{11}+F^{\text{hom}}{}_{11}K_{111} \\ S_{111} &= B^{\text{hom}}{}_{11}E_{11}+A^{\text{hom}}{}_{11}K_{111} \\ R_{11} &= e^{\text{hom}}{}_{11}E_{11}+H^{\text{hom}}{}_{11}K_{111} \end{aligned} \tag{56}$$

Considering the case of the first gradient medium, the constitutive law is written in terms of the first gradient rigidity matrix (here composed of $C^{\text{hom}}{}_{11}$ only), Eq. (57), i.e. without taking into account the term related to the second gradient, namely $B^{\text{hom}}{}_{11}$. The resulting macroscopic deformation is equal to a constant and it is moreover independent of the position (Fig. 6):

$$\Sigma_{11} = \Sigma_0 = C^{\text{hom}}{}_{11}E_{11} \rightarrow E_{11} = \frac{\Sigma_0}{C^{\text{hom}}{}_{11}} \tag{57}$$

To the contrary, if we take into consideration the second gradient parameter, the macroscopic deformation is no more constant and it depends on the position from the fixed left end of the beam. In this case, the deformation increases expo-

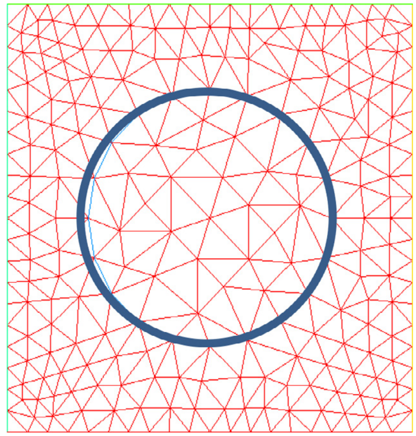

Fig. 7. Meshed composite microstructure with circular inclusion and square matrix. The unit cell has a linear unit length. The volume fraction of inclusion is 0.3.

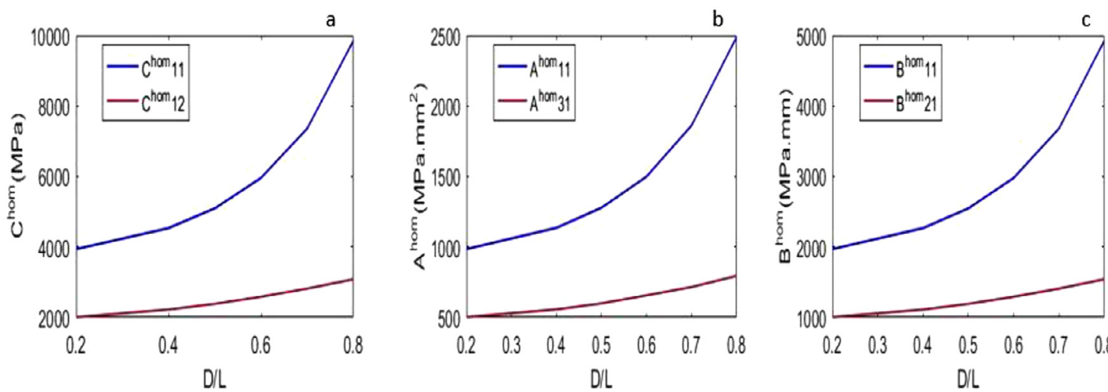

Fig. 8. Homogenized (a) First gradient rigidity coefficients, (b) Second gradient rigidity coefficients, (c) Second gradient coupling terms.

nentially from the selected nil strain boundary condition at the fixed support (incompatible with the Cauchy-type, pure first gradient solution), as shown in Fig. 5, revealing a boundary layer in the vicinity of the left edge of the beam:

$$\Sigma_{11} = \Sigma_0 = C^{hom}{}_{11}E_{11} + B^{hom}{}_{11}\frac{dE_{11}}{dx} \rightarrow E_{11} = \frac{\Sigma_0}{C^{hom}{}_{11}}\left(1 - \exp^{-\frac{C^{hom}{}_{11}}{B^{hom}{}_{11}}x}\right) \tag{58}$$

6. Effective flexoelectric properties of inclusion based piezoelectric planar composites

We subsequently employ the methodology elaborated in Sections 2 and 3 and the algorithm described in Section 4 to compute the effective homogenized properties of a piezoelectric composite consisting of two piezoelectric materials, namely $LiNbO_3$ for the inclusion (a fiber) and Polyfluorure of Vinylidene (PVDF in short) used as the matrix phase. The meshed geometrical domain is shown in Fig. 7 and the properties of both constituents are listed in Table 1. The volumetric percentage of $LiNbO_3$ within the unit cell is characterized by the parameter ν_f (here ν_f=0.3).

The first parameter of interest, influencing the homogenized properties, is the volume fraction of inclusion which is studied by changing the inclusion diameter D (the fiber domain is the circle, the matrix domain is the square in Fig. 7 and L is the unit cell linear length). The second parameter is the ratio of fiber to matrix tensile moduli, Ef/Em. Fig. 8 through 11 show the variation of the homogenized moduli with the fiber diameter.

The homogenized coefficients of the first gradient rigidity matrix ($C^{hom}{}_{11}$, $C^{hom}{}_{12}$), the second gradient rigidity matrix ($A^{hom}{}_{11}$, $A^{hom}{}_{31}$), and the coupling matrix ($B^{hom}{}_{11}$, $B^{hom}{}_{21}$) shown in Fig. 6, increase with the fiber diameter; the increase is due to the corresponding increase in the relative amount of the more rigid phase (fiber).

In the graphs of Fig. 9, the coefficients $d^{hom}{}_{11}$, $e^{hom}{}_{11}$, and $H^{hom}{}_{11}$ decrease slightly with the fiber's diameter, while $d^{hom}{}_{21}$, $e^{hom}{}_{12}$, and $H^{hom}{}_{12}$ increase slightly. The coefficients $eD^{hom}{}_{11}$, $eD^{hom}{}_{23}$, $N^{hom}{}_{11}$, and $N^{hom}{}_{33}$ in Fig. 10 are increasing as a function of the ratio D/L. The permittivity coefficients $a^{hom}{}_{11}$, $a^{hom}{}_{22}$ in Fig. (11i) are also increasing with the diameter of the fiber, due to the increasing percentage of the fiber phase (LiNbo3) having the higher values of permittivity (a_{11}, a_{22}). Also, in figure (11j), the coefficients $F^{hom}{}_{22}$, and $F^{hom}{}_{23}$ increase slightly as the diameter of the fiber increases.

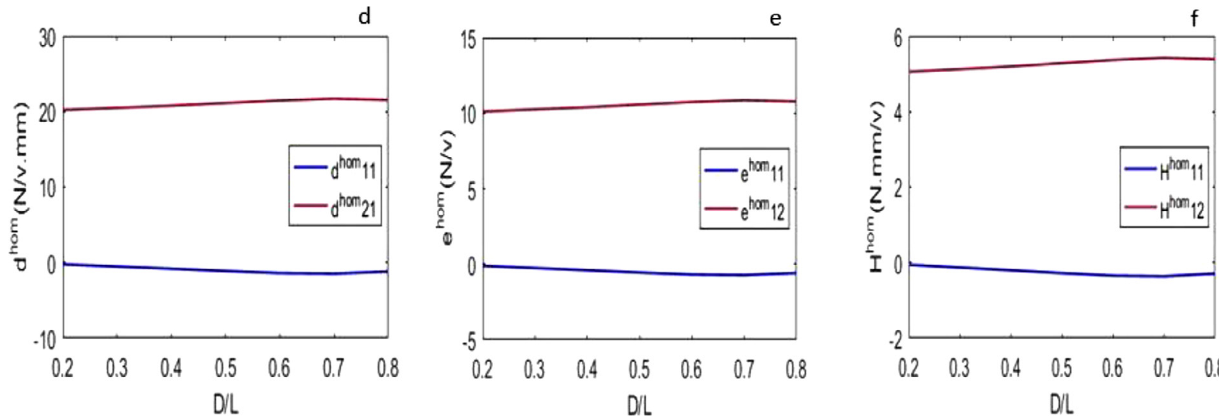

Fig. 9. Homogenized (d) piezoelectric coefficients d^{hom}, (e) coupling coefficients e^{hom}, (f) coupling terms H^{hom}.

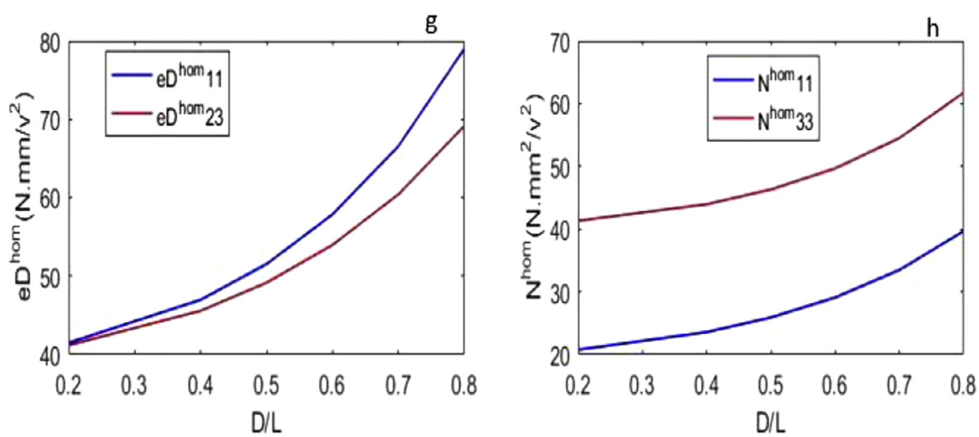

Fig. 10. Homogenized (g) coupling term eD^{hom} and (h) coupling term N^{hom}.

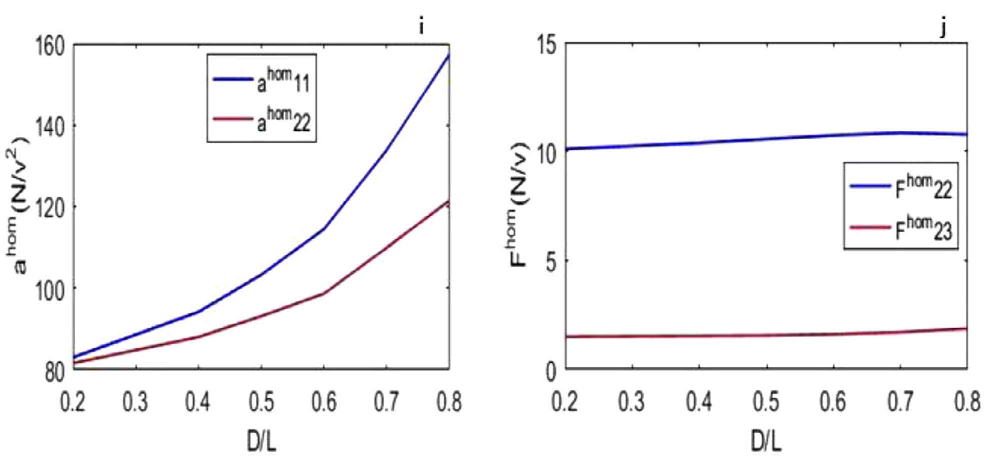

Fig. 11. Homogenized (i) permittivity coefficients a^{hom}, (j) coupling coefficients F^{hom}.

A comparison with the results obtained in Sevostianov and Sabina (2007) shows a good agreement for the piezoelectric and dielectric coefficients with maximum relative error for the piezoelectric coefficient 3% and for the dielectric coefficient (permittivity) around 1% (see Appendix B).

Fig. 12 shows the variation of some homogenized coefficients as a function of the ratio of fiber to matrix Young moduli. Fig. 12 shows that the first gradient and second gradient rigidity coefficients $C^{hom}{}_{11}$, $C^{hom}{}_{12}$, and $A^{hom}{}_{11}$, $A^{hom}{}_{12}$ respectively increase rapidly up to a ratio close to 10, beyond which they remain constant. In Fig. 13, the permittivity coefficient $a^{hom}{}_{22}$, and the coefficient $N^{hom}{}_{22}$ decrease rapidly for a ratio of moduli close to 10. Conversely, $a^{hom}{}_{11}$ and $N^{hom}{}_{11}$ remain constant for all moduli ratios.

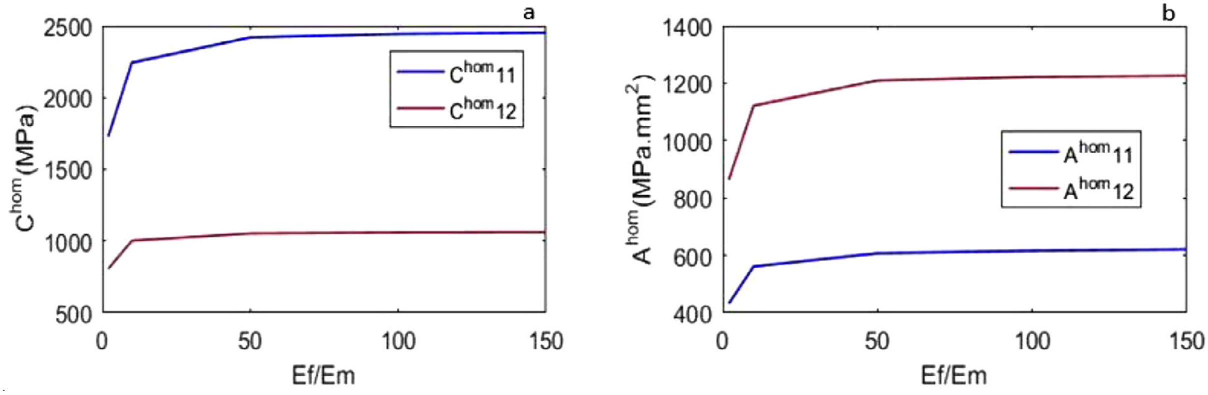

Fig. 12. Variation of the first gradient rigidity coefficients (a), and second gradient rigidity coefficients (b) versus the ratio of fiber to matrix Young moduli Ef/Em.

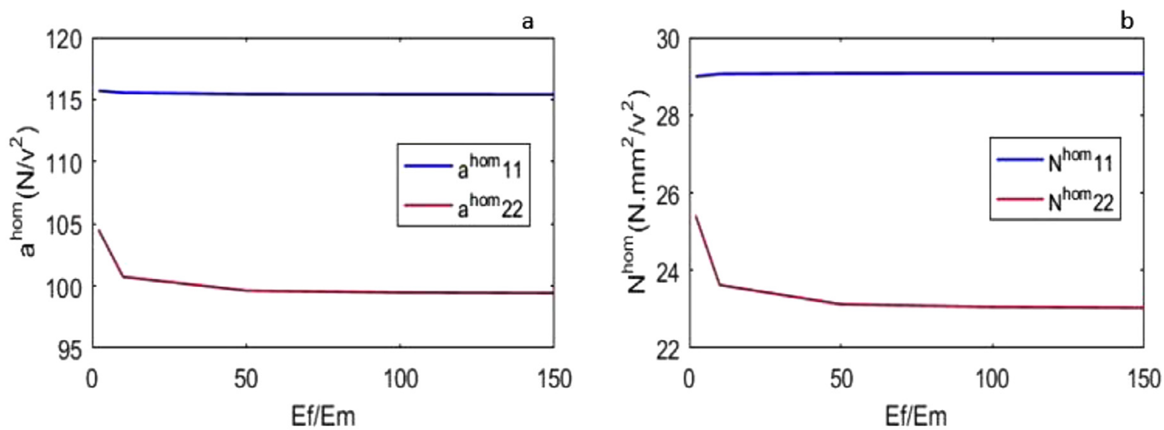

Fig. 13. Variation of the permittivity coefficients (a), and coefficients of N^{hom} matrix (b) versus the ratio of fiber to matrix Young moduli Ef/Em.

The internal lengths are defined in full generality as the ratio between second gradient to first gradient coefficients for the different deformation modes; they quantify the strengths of strain gradient phenomena relative to first gradient ones. For mechanics, the internal lengths express in terms of the rigidity coefficients as (the superscript s refers to the static case)

$$l_{xx}^{s} = \sqrt{\frac{A_{11}^{hom}}{C_{11}^{hom}}},\ l_{xy}^{s} = \sqrt{\frac{A_{12}^{hom}}{C_{12}^{hom}}} \tag{59}$$

These lengths in extension and shear remain nearly constant over the considered range of moduli ratio, with a value about one-half that of the unit cell size. This indicates that the first and second gradient effects equally contribute to the internal length in terms of their sensitivity to the mechanical properties of the individual composite constituents.

The internal lengths for electrical phenomena (described by superscript E) express as the ratio of flexoelectric and permittivity coefficients as

$$l_{xx}^{E} = \sqrt{\frac{N_{11}^{hom}}{a_{11}^{hom}}},\ l_{yy}^{E} = \sqrt{\frac{N_{22}^{hom}}{a_{22}^{hom}}} \tag{60}$$

l_{xx}^{E} and l_{yy}^{E} are found to be constant with a value around one-half. This shows that the internal lengths associated to electrical phenomena are approximately the same as those of mechanical phenomena quantified by the internal lengths l_{xx}^{s}, l_{xy}^{s}.

The distribution of the fluctuating displacement and electric fields along a vertical line passing through the fibers is represented for one and four unit cells when applying **E** and **K** as kinematic loads over the unit cell. Fig. 14 shows 4-unit cells in which a vertical line passes through the center of the fibers. The fluctuating vertical displacement $\tilde{u}_y$ is plotted along the vertical line with the microscopic position y varying from 0 to 1.

Fig. 15 shows the variation of the vertical component $\tilde{u}_y$ along the vertical line for 1 and 4 unit cells when applying the strain and strain gradient components $E_{11}=1$, and $K_{111}=1$ respectively for the flexoelectric medium.

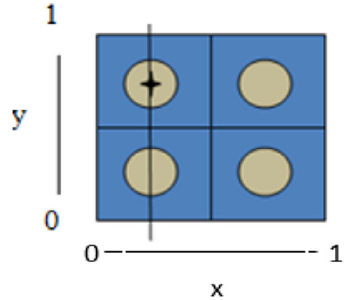

Fig. 14. four unit cells with a vertical line passing through the center of fibers.

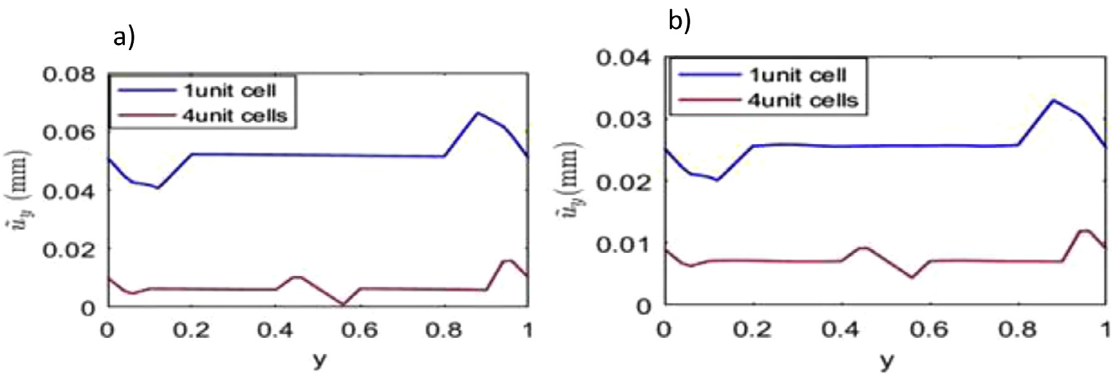

Fig. 15. Distribution of the fluctuating displacement $\tilde{u}_y$ (in mm) on the vertical axis, due to the macroscopic strain (a) $E_{11} = 1$, and (b) $K_{111} = 1$ along a vertical line through the centers of the inclusions.

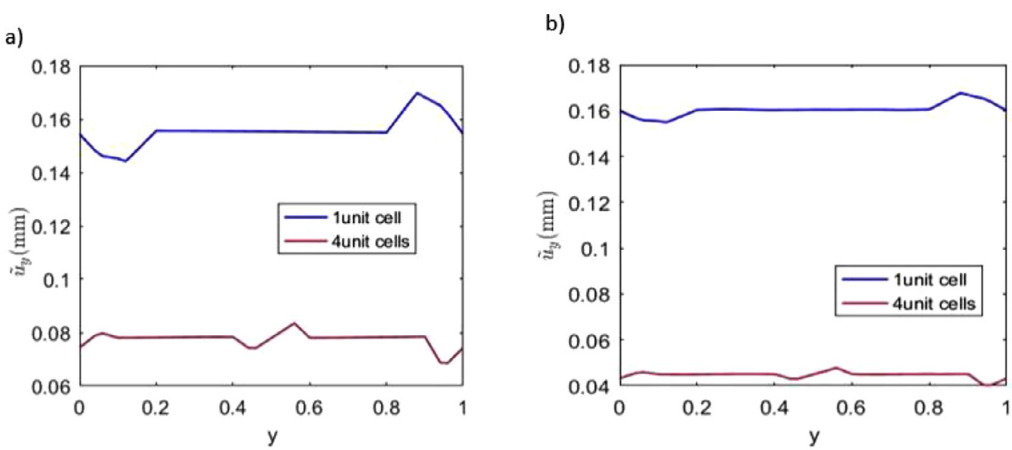

Fig. 16. Distribution of the fluctuating displacement $\tilde{u}_y$ (in mm), due to the macroscopic strain component $E_{11} = 1$, and b) strain gradient component $K_{111} = 1$ along a vertical line through the centers of the inclusions for the pure elastic medium with no electric effects.

Fig. 15 shows that for four unit cells, the fluctuating displacement $\tilde{u}_y$ is repeating the pattern obtained for a single unit cell. The displacement $\tilde{u}_y$ appears to be nearly constant far away from the interface (in the fiber). Strong displacement variations are indicators of the existence of the interface between fiber and matrix.

In Fig. 16, the fluctuating displacement $\tilde{u}_y$ for four unit cells, is repeating the pattern of a single unit cell, but with a lower amplitude. The values of $\tilde{u}_y$ obtained (in case of four unit cells) are of negative sign but they are plotted using their absolute value.

The values of $\tilde{u}_y$ for a single unit cell determined when applying the strain component E_{11} are approximately twice the values of $\tilde{u}_y$ for four unit cells (number of vertical cells as shown in Fig. 14); they will become identical when a normalization by the number of unit cells is applied. Meanwhile, the values of $\tilde{u}_y$ for a single unit cell, determined when applying the strain gradient component K_{111}, are approximately four times the values of $\tilde{u}_y$ for four unit cells. It is observed that the spatial distribution of the microscopic fluctuation under the applied macroscopic deformation $E_{11} = 1$ remains the same in each case, repeating the pattern obtained for a single unit (the factor 2 corresponding to the number of unit cells) cell over the neighboring (internal) unit cells. Consequently, the Cauchy homogenized elastic coefficients remain unchanged for computations done with one or a multiple number of periods, since the spatial distribution of the fluctuating displacement does not depend on the unit cell.

The constant values of $\tilde{u}_y$ in Fig. 16 are related to the position of the fiber; one can thus predict the diameter of the fiber from the figures where there is a constant line (for example, from Fig. 16, for 1-unit cell: the diameter value is 0.8-0.2=0.6). The effective piezoelectric and flexoelectric coefficients remain constant – thus independent of unit cell size - when normalized by the square of the number of unit cells.

7. Conclusion

The effective linear piezoelectric properties of heterogeneous materials have been evaluated in full generality in the context of periodic homogenization, employing a variational formulation in combination with the extended Hill macro-homogeneity condition. The microscopic variables – the displacement and polarization vectors – have been expressed as the sum of a homogeneous part and a fluctuation obeying a minimum principle. The entire set of homogenized moduli has been obtained, expressing as volumetric averages of the microscopic properties of the individual constituents weighted by the displacement and polarization localization operators.

This framework has been extended in a second part of the paper to the computation of the effective flexoelectric properties, thereby accounting for higher gradient effects that may be induced by a strong contrast of properties of the composite constituents. The effective properties of inclusion-based composites have been evaluated numerically as an application of the proposed general homogenization framework, and the effect of the volume fraction and relative tensile modulus of the reinforcement versus the one of the matrix phase has been assessed. Computations show especially that the internal lengths associated to electrical phenomena are higher than the internal lengths of mechanical phenomena.

The proposed homogenization method has given rise to a finite element implementation for the efficient computation of the effective flexoelectric properties of composites in a broad sense. This numerical platform is convenient to investigate in future contributions the flexoelectric properties of architectured materials or diverse classes of composite materials.

Declaration of Competing Interest

None.

Acknowledgments

V.A.E. acknowledges the support by grant 14.Z50.31.0036 awarded to R. E. Alekseev Nizhny Novgorod Technical University by Department of Education and Science of the Russian Federation.

Appendix A

The factorization of Eq. (16) leads to the following expression of the macroscopic stress:

$$\begin{aligned}
\boldsymbol{\Sigma} &= \frac{1}{2}\int_Y \left\{ \begin{array}{l}
\left(\mathbf{E}+\mathbf{M}^{uE}\otimes\nabla_y:\mathbf{E}+\mathbf{M}^{uP}\otimes\nabla_y.\mathbf{E}_{\mathbf{M}}^{\mathbf{elec}}\right):\mathbf{C}:\left(\mathbf{I}_4+\mathbf{M}^{uE}\otimes\nabla_y\right)\\
+\left(\mathbf{I}_4+\mathbf{M}^{uE}\otimes\nabla_y\right):\mathbf{C}:\left(\mathbf{E}+\mathbf{M}^{uE}\otimes\nabla_y:\mathbf{E}+\mathbf{M}^{uP}\otimes\nabla_y.\mathbf{E}_{\mathbf{M}}^{\mathbf{elec}}\right)\\
+\left(\mathbf{E}_{\mathbf{M}}^{\mathbf{elec}}+\mathbf{M}^{PE}(\mathbf{y}):\mathbf{E}+\mathbf{M}^{PP}.\mathbf{E}_{\mathbf{M}}^{\mathbf{elec}}\right).\mathbf{a}.\mathbf{M}^{PE}+\mathbf{M}^{PE}.\mathbf{a}.\left(\mathbf{E}_{\mathbf{M}}^{\mathbf{elec}}+\mathbf{M}^{PE}:\mathbf{E}+\mathbf{M}^{PP}.\mathbf{E}_{\mathbf{M}}^{\mathbf{elec}}\right)\\
+\left(\mathbf{I}_4+\mathbf{M}^{uE}\otimes\nabla_y\right).\mathbf{d}.\left(\mathbf{P}+\mathbf{M}^{PE}:\mathbf{E}+\mathbf{M}^{PP}.\mathbf{E}_{\mathbf{M}}^{\mathbf{elec}}\right)+\left(\mathbf{E}+\mathbf{M}^{uE}\otimes\nabla_y:\mathbf{E}+\mathbf{M}^{uP}\otimes\nabla_y.\mathbf{E}_{\mathbf{M}}^{\mathbf{elec}}\right).\mathbf{d}.\mathbf{M}^{PE}\\
+\mathbf{M}^{PE}.\mathbf{d}.\left(\mathbf{E}+\mathbf{M}^{uE}\otimes\nabla_y:\mathbf{E}+\mathbf{M}^{uP}\otimes\nabla_y.\mathbf{E}_{\mathbf{M}}^{\mathbf{elec}}(\mathbf{x})\right)+\left(\mathbf{E}_{\mathbf{M}}^{\mathbf{elec}}+\mathbf{M}^{PE}:\mathbf{E}+\mathbf{M}^{PP}.\mathbf{E}_{\mathbf{M}}^{\mathbf{elec}}\right).\mathbf{d}.\left(\mathbf{I}_4+\mathbf{M}^{uE}\otimes\nabla_y\right)
\end{array}\right\} dV_y\\
&+\frac{1}{2}\int_Y \left(\begin{array}{l}
\left(\mathbf{I}_4+\mathbf{M}^{uE}\otimes\nabla_y\right)^T:\mathbf{C}:\left(\mathbf{I}_4+\mathbf{M}^{uE}\otimes\nabla_y\right)+\left(\mathbf{I}_4+\mathbf{M}^{uE}\otimes\nabla_y\right):\mathbf{C}:\left(\mathbf{I}_4+\mathbf{M}^{uE}\otimes\nabla_y\right)\\
+\left(\mathbf{M}^{PE}\right)^T.\mathbf{a}.\mathbf{M}^{PE}+\mathbf{M}^{PE}.\mathbf{a}.\left(\mathbf{M}^{PE}\right)+\left(\mathbf{I}_4+\mathbf{M}^{uE}\otimes\nabla_y\right).\mathbf{d}.\mathbf{M}^{PE}+\left(\mathbf{I}_4+\mathbf{M}^{uE}\otimes\nabla_y\right)^T.\mathbf{d}.\mathbf{M}^{PE}+\\
+\mathbf{M}^{PE}.\mathbf{d}.\left(\mathbf{I}_4+\mathbf{M}^{uE}\otimes\nabla_y\right)+\left(\mathbf{M}^{PE}\right)^T.\mathbf{d}.\left(\mathbf{I}_4+\mathbf{M}^{uE}\otimes\nabla_y\right)
\end{array}\right):\mathbf{E}\,dV_y\\
&=\frac{1}{2}\int_Y \left(\begin{array}{l}
\left(\mathbf{M}^{uP}\otimes\nabla_y\right)^T:\mathbf{C}:\left(\mathbf{I}_4+\mathbf{M}^{uE}\otimes\nabla_y\right)+\left(\mathbf{I}_4+\mathbf{M}^{uE}\otimes\nabla_y\right):\mathbf{C}:\left(\mathbf{M}^{uP}\otimes\nabla_y\right)+\left(\mathbf{I}_2+\mathbf{M}^{PP}\right)^T.\mathbf{a}.\mathbf{M}^{PE}\\
+\mathbf{M}^{PE}.\mathbf{a}.\left(\mathbf{I}_2+\mathbf{M}^{PP}\right)+\left(\mathbf{I}_4+\mathbf{M}^{uE}\otimes\nabla_y\right).\mathbf{d}.\left(\mathbf{I}_2+\mathbf{M}^{PP}\right)\\
+\left(\mathbf{M}^{uP}\otimes\nabla_y\right)^T.\mathbf{d}.\mathbf{M}^{PE}+\mathbf{M}^{PE}.\mathbf{d}.\left(\mathbf{M}^{uP}\otimes\nabla_y\right)+\left(\mathbf{I}_2+\mathbf{M}^{PP}\right)^T\mathbf{d}.\left(\mathbf{I}_4+\mathbf{M}^{uE}\otimes\nabla_y\right)
\end{array}\right).\mathbf{E}_{\mathbf{M}}^{\mathbf{elec}}\,dV_y
\end{aligned} \tag{A.1}$$

Similarly, by factorizing Eq. (17), the electric displacement satisfies the following constitutive relation:

$$\overline{\mathbf{D}}=\frac{1}{2}\int_Y \left\{\begin{array}{l}
\left(\mathbf{M}^{uP}\otimes\nabla_y\right):\mathbf{C}:\left(\mathbf{E}+\mathbf{M}^{uE}\otimes\nabla_y:\mathbf{E}+\mathbf{M}^{uP}\otimes\nabla_y.\mathbf{E}_{\mathbf{M}}^{\mathbf{elec}}\right)\\
+\left(\mathbf{E}+\mathbf{M}^{uE}\otimes\nabla_y:\mathbf{E}+\mathbf{M}^{uP}\otimes\nabla_y.\mathbf{E}_{\mathbf{M}}^{\mathbf{elec}}\right):\mathbf{C}:(\mathbf{M}^{uP}\otimes\nabla_y)\\
+\left(\mathbf{I}_2+\mathbf{M}^{PP}\right).\mathbf{a}.\left(\mathbf{E}_{\mathbf{M}}^{\mathbf{elec}}+\mathbf{M}^{PE}:\mathbf{E}+\mathbf{M}^{PP}.\mathbf{E}_{\mathbf{M}}^{\mathbf{elec}}\right)+\left(\mathbf{E}_{\mathbf{M}}^{\mathbf{elec}}+\mathbf{M}^{PE}:\mathbf{E}+\mathbf{M}^{PP}.\mathbf{E}_{\mathbf{M}}^{\mathbf{elec}}\right).\mathbf{a}.\left(\mathbf{I}_2+\mathbf{M}^{PP}\right)\\
+\left(\mathbf{M}^{uP}\otimes\nabla_y\right).\mathbf{d}.\left(\mathbf{E}_{\mathbf{M}}^{\mathbf{elec}}+\mathbf{M}^{PE}:\mathbf{E}+\mathbf{M}^{PP}.\mathbf{E}_{\mathbf{M}}^{\mathbf{elec}}\right)+\left(\mathbf{E}+\mathbf{M}^{uE}\otimes\nabla_y:\mathbf{E}+\mathbf{M}^{uP}\otimes\nabla_y.\mathbf{E}_{\mathbf{M}}^{\mathbf{elec}}\right).\mathbf{d}.\left(\mathbf{I}_2+\mathbf{M}^{PP}\right)\\
+\left(\mathbf{I}_2+\mathbf{M}^{PP}\right).\mathbf{d}.\left(\mathbf{E}+\mathbf{M}^{uE}\otimes\nabla_y:\mathbf{E}+\mathbf{M}^{uP}\otimes\nabla_y.\mathbf{E}_{\mathbf{M}}^{\mathbf{elec}}\right)+\left(\mathbf{E}_{\mathbf{M}}^{\mathbf{elec}}+\mathbf{M}^{PE}:\mathbf{E}+\mathbf{M}^{PP}.\mathbf{E}_{\mathbf{M}}^{\mathbf{elec}}\right).\mathbf{d}.\left(\mathbf{M}^{uP}\otimes\nabla_y\right)
\end{array}\right\} dV_y$$

$$= \frac{1}{2}\int_Y \begin{pmatrix} (\mathbf{M}^{uP}\otimes\nabla_y) : \mathbf{C}(\mathbf{y}) : (\mathbf{I}_4 + \mathbf{M}^{uE}\otimes\nabla_y) + (\mathbf{I}_4 + \mathbf{M}^{uE}\otimes\nabla_y)^T : \mathbf{C} : (\mathbf{M}^{uP}\otimes\nabla_y) \\ +(\mathbf{I}_2 + \mathbf{M}^{PP}).\mathbf{a}.\mathbf{M}^{PE} + (\mathbf{M}^{PE})^T.\mathbf{a}.(\mathbf{I}_2 + \mathbf{M}^{PP}) \\ +(\mathbf{M}^{uP}\otimes\nabla_y).\mathbf{d}.\mathbf{M}^{PE} + (\mathbf{I}_4 + \mathbf{M}^{uE}\otimes\nabla_y)^T.\mathbf{d}.(\mathbf{I}_2 + \mathbf{M}^{PP}) \\ +(\mathbf{I}_2 + \mathbf{M}^{PP}).\mathbf{d}.(\mathbf{I}_4 + \mathbf{M}^{uE}\otimes\nabla_y) + (\mathbf{M}^{PE})^T.\mathbf{d}.(\mathbf{M}^{uP}\otimes\nabla_y) \end{pmatrix} : \mathbf{E}\, dV_y$$
$$+\frac{1}{2}\int_Y \begin{pmatrix} (\mathbf{M}^{uP}\otimes\nabla_y)\mathbf{C} : (\mathbf{M}^{uP}\otimes\nabla_y) + (\mathbf{M}^{uP}\otimes\nabla_y)^T : \mathbf{C} : (\mathbf{M}^{uP}\otimes\nabla_y) + (\mathbf{I}_2 + \mathbf{M}^{PP}).\mathbf{a}.(\mathbf{I}_2 + \mathbf{M}^{PP}) + (\mathbf{I}_2 + \mathbf{M}^{PP})^T.\mathbf{a}.(\mathbf{I}_2 + \mathbf{M}^{PP}) \\ +(\mathbf{M}^{uP}\otimes\nabla_y).\mathbf{d}.(\mathbf{I}_2 + \mathbf{M}^{PP}) + (\mathbf{M}^{uP}\otimes\nabla_y)^T.\mathbf{d}.(\mathbf{I}_2 + \mathbf{M}^{PP}) + (\mathbf{I}_2 + \mathbf{M}^{PP}).\mathbf{d}.(\mathbf{M}^{uP}\otimes\nabla_y) + (\mathbf{I}_2 + \mathbf{M}^{PP})^T.\mathbf{d}.(\mathbf{M}^{uP}\otimes\nabla_y) \end{pmatrix}.\mathbf{E}_{\mathbf{M}}^{\mathbf{elec}}\, dV_y \tag{A.2}$$

Comparing Eq. (18) with Eqs. (A.1) and (A.2), the expressions of $\mathbf{C}^{\text{hom}}$, $\mathbf{d}^{\text{hom}}$, and $\mathbf{a}^{\text{hom}}$ are obtained as follows:

$$\mathbf{C}^{\text{hom}} := \frac{1}{2}\int_Y \begin{pmatrix} (\mathbf{I}_4 + \mathbf{M}^{uE}\otimes\nabla_y)^T : \mathbf{C} : (\mathbf{I}_4 + \mathbf{M}^{uE}\otimes\nabla_y) \\ +(\mathbf{I}_4 + \mathbf{M}^{uE}\otimes\nabla_y) : \mathbf{C} : (\mathbf{I}_4 + \mathbf{M}^{uE}\otimes\nabla_y) + (\mathbf{M}^{PE})^T.\mathbf{a}.\mathbf{M}^{PE} \\ +\mathbf{M}^{PE}.\mathbf{a}.\mathbf{M}^{PE} + (\mathbf{I}_4 + \mathbf{M}^{uE}\otimes\nabla_y)^T.\mathbf{d}.\mathbf{M}^{PE} + (\mathbf{I}_4 + \mathbf{M}^{uE}\otimes\nabla_y)^T.\mathbf{d}.\mathbf{M}^{PE} \\ +\mathbf{M}^{PE}.\mathbf{d}.(\mathbf{I}_4 + \mathbf{M}^{uE}\otimes\nabla_y) + (\mathbf{M}^{PE})^T.\mathbf{d}.(\mathbf{I}_4 + \mathbf{M}^{uE}\otimes\nabla_y) \end{pmatrix} dV_y \tag{A.3}$$

$$\mathbf{d}^{\text{hom}} := \frac{1}{2}\int_Y \begin{pmatrix} (\mathbf{M}^{uP}\otimes\nabla_y)^T : \mathbf{C} : (\mathbf{I}_4 + \mathbf{M}^{uE}\otimes\nabla_y) \\ +(\mathbf{I}_4 + \mathbf{M}^{uE}\otimes\nabla_y) : \mathbf{C} : (\mathbf{M}^{uP}\otimes\nabla_y) + (\mathbf{I}_2 + \mathbf{M}^{PP})^T.\mathbf{a}.\mathbf{M}^{PE} \\ +\mathbf{M}^{PE}.\mathbf{a}.(\mathbf{I}_2 + \mathbf{M}^{PP}) + (\mathbf{I}_4 + \mathbf{M}^{uE}\otimes\nabla_y).\mathbf{d}.(\mathbf{I}_2 + \mathbf{M}^{PP}) \\ +(\mathbf{M}^{uP}\otimes\nabla_y)^T.\mathbf{d}.\mathbf{M}^{PE} + \mathbf{M}^{PE}.\mathbf{d}.(\mathbf{M}^{uP}\otimes\nabla_y) + (\mathbf{I}_2 + \mathbf{M}^{PP})^T\mathbf{d}.(\mathbf{I}_4 + \mathbf{M}^{uE}\otimes\nabla_y) \end{pmatrix} dV_y$$

$$\mathbf{a}^{\text{hom}} := \frac{1}{2}\int_Y \begin{pmatrix} (\mathbf{M}^{uP}\otimes\nabla_y)\mathbf{C} : (\mathbf{M}^{uP}\otimes\nabla_y) + (\mathbf{M}^{uP}\otimes\nabla_y)^T : \mathbf{C} : (\mathbf{M}^{uP}\otimes\nabla_y) + (\mathbf{I}_2 + \mathbf{M}^{PP}).\mathbf{a}.(\mathbf{I}_2 + \mathbf{M}^{PP}) \\ +(\mathbf{I}_2 + \mathbf{M}^{PP})^T.\mathbf{a}.(\mathbf{I}_2 + \mathbf{M}^{PP}) + (\mathbf{M}^{uP}\otimes\nabla_y).\mathbf{d}.(\mathbf{I}_2 + \mathbf{M}^{PP}) + (\mathbf{M}^{uP}\otimes\nabla_y)^T.\mathbf{d}.(\mathbf{I}_2 + \mathbf{M}^{PP}) \\ +(\mathbf{I}_2 + \mathbf{M}^{PP}).\mathbf{d}.(\mathbf{M}^{uP}\otimes\nabla_y) + (\mathbf{I}_2 + \mathbf{M}^{PP})^T.\mathbf{d}.(\mathbf{M}^{uP}\otimes\nabla_y) \end{pmatrix} dV_y$$

On the other hand these homogenized tensors can be written in terms of more compact localizators (the strain localizators ($\mathbf{Z^{uE}}$, $\mathbf{Z^{PE}}$) and polarization localizators ($\mathbf{Z^{uP}}$, $\mathbf{Z^{PP}}$)) where:

$$\left| \begin{array}{l} \mathbf{u}(\mathbf{y})\otimes\nabla_y = (\mathbf{u}^{\text{hom}}(\mathbf{y}) + \tilde{\mathbf{u}}(\mathbf{y}))\otimes\nabla_y := \mathbf{E}(\mathbf{x}) + \mathbf{M}^{uE}(\mathbf{y})\otimes\nabla_y : \mathbf{E}(\mathbf{x}) + \mathbf{M}^{uP}(\mathbf{y})\otimes\nabla_y.\mathbf{E}_{\mathbf{M}}^{\mathbf{elec}}(\mathbf{x}) \\ \equiv \mathbf{Z}^{uE}(\mathbf{y}) : \mathbf{E}(\mathbf{x}) + \mathbf{Z}^{uP}(\mathbf{y}).\mathbf{E}_{\mathbf{M}}^{\mathbf{elec}}(\mathbf{x}) \\ \mathbf{Z}^{uE}(\mathbf{y}) = (\mathbf{I}_4 + \mathbf{M}^{uE}\otimes\nabla_y) \\ \mathbf{Z}^{uP}(\mathbf{y}) = (\mathbf{M}^{uP}\otimes\nabla_y) \\ \mathbf{E}^{elec} = \mathbf{E}_{\mathbf{M}}^{\mathbf{elec}} + \tilde{\mathbf{E}}^{elec}(\mathbf{y}) = \mathbf{M}^{PE}(\mathbf{y}) : \mathbf{E}(\mathbf{x}) + \mathbf{E}_{\mathbf{M}}^{\mathbf{elec}} + \mathbf{M}^{PP}(\mathbf{y}).\mathbf{E}_{\mathbf{M}}^{\mathbf{elec}}(\mathbf{x}) \equiv \mathbf{Z^{PE}}(\mathbf{y}) : \mathbf{E}(\mathbf{x}) + \mathbf{Z^{PP}}(\mathbf{y}).\mathbf{E}_{\mathbf{M}}^{\mathbf{elec}}(\mathbf{x}) \\ \mathbf{Z^{PE}}(y) = \mathbf{M}^{PE}(\mathbf{y}) \\ \mathbf{Z^{PP}}(\mathbf{y}) = (\mathbf{I}_2 + \mathbf{M}^{PP}(\mathbf{y})) \end{array} \right. \tag{A.4}$$

Eq. (18) leads to the constitutive law, in terms of the strain and polarization localizators, as follows:

$$\mathbf{\Sigma} = \underset{\tilde{\mathbf{u}},\tilde{\phi}\in H^1_{per}(Y)}{Min} \frac{\partial L[\tilde{\mathbf{u}},\tilde{\phi}]}{\partial E}$$
$$= \frac{1}{2}\int_Y \left\{ \begin{array}{l} (\mathbf{Z^{uE}}) : \mathbf{C} : (\mathbf{Z^{uE}} : \mathbf{E} + \mathbf{Z^{uP}}.\mathbf{E}_{\mathbf{M}}^{\mathbf{elec}}) + (\mathbf{Z^{uE}} : \mathbf{E} + \mathbf{Z^{uP}}.\mathbf{E}_{\mathbf{M}}^{\mathbf{elec}}) : \mathbf{C} : (\mathbf{Z^{uE}}) \\ +(\mathbf{Z^{PE}}).\mathbf{a}.(\mathbf{Z^{PE}} : \mathbf{E} + \mathbf{Z^{PP}}.\mathbf{E}_{\mathbf{M}}^{\mathbf{elec}}) + (\mathbf{Z^{PE}} : \mathbf{E} + \mathbf{Z^{PP}}.\mathbf{E}_{\mathbf{M}}^{\mathbf{elec}}).\mathbf{a}.(\mathbf{Z^{PE}}) \\ +(\mathbf{Z^{uE}}).\mathbf{d}.(\mathbf{Z^{PE}} : \mathbf{E} + \mathbf{Z^{PP}}.\mathbf{E}_{\mathbf{M}}^{\mathbf{elec}}) + (\mathbf{Z^{uE}} : \mathbf{E} + \mathbf{Z^{uP}}.\mathbf{E}_{\mathbf{M}}^{\mathbf{elec}}).\mathbf{d}.(\mathbf{Z^{PE}}) \\ +(\mathbf{Z^{PE}}).\mathbf{d}.(\mathbf{Z^{uE}} : \mathbf{E} + \mathbf{Z^{uP}}.\mathbf{E}_{\mathbf{M}}^{\mathbf{elec}}) + (\mathbf{Z^{PE}} : \mathbf{E} + \mathbf{Z^{PP}}.\mathbf{E}_{\mathbf{M}}^{\mathbf{elec}}).\mathbf{d}.(\mathbf{Z^{uE}}) \end{array} \right\} dV_y$$
$$= \frac{1}{2}\left(\int_Y \left\{ \begin{array}{l} (\mathbf{Z^{uE}}) : \mathbf{C} : \mathbf{Z^{uE}} + (\mathbf{Z^{uE}})^{\mathbf{T}} : \mathbf{C} : \mathbf{Z^{uE}} + (\mathbf{Z^{PE}}).\mathbf{a}.\mathbf{Z^{PE}} + (\mathbf{Z^{PE}})^T.\mathbf{a}.\mathbf{Z^{PE}} \\ +(\mathbf{Z^{uE}}).\mathbf{d}.\mathbf{Z^{PE}} + (\mathbf{Z^{uE}})^{\mathbf{T}}.\mathbf{d}.\mathbf{Z^{PE}} + (\mathbf{Z^{PE}}).\mathbf{d}.\mathbf{Z^{uE}} + (\mathbf{Z^{PE}})^{\mathbf{T}}.\mathbf{d}.\mathbf{Z^{uE}} \end{array} \right\} dV_y \right) : \mathbf{E}$$
$$+\frac{1}{2}\left(\int_Y \left\{ \begin{array}{l} (\mathbf{Z^{uE}}) : \mathbf{C} : (\mathbf{Z^{uP}}) + (\mathbf{Z^{uP}})^T : \mathbf{C} : (\mathbf{Z^{uE}}) + (\mathbf{Z^{PE}}).\mathbf{a}.(\mathbf{Z^{PP}}) + (\mathbf{Z^{PP}})^T.\mathbf{a}.(\mathbf{Z^{PE}}) \\ +(\mathbf{Z^{uE}}).\mathbf{d}.(\mathbf{Z^{PP}}) + (\mathbf{Z^{uP}})^T.\mathbf{d}.(\mathbf{Z^{PE}}) + (\mathbf{Z^{PE}}).\mathbf{d}.(\mathbf{Z^{uP}}) + (\mathbf{Z^{PP}})^T.\mathbf{d}.(\mathbf{Z^{uE}}) \end{array} \right\} dV_y \right).\mathbf{E}_{\mathbf{M}}^{\mathbf{elec}}$$

$$\overline{\mathbf{D}} = \underset{\tilde{\mathbf{u}},\tilde{\phi}\in H^1_{per}(Y)}{Min} \frac{\partial L[\tilde{\mathbf{u}},\tilde{\phi}]}{\partial \mathbf{E}_{\mathbf{M}}^{\mathbf{elec}}}$$
$$= \frac{1}{2}\int_Y \left\{ \begin{array}{l} (\mathbf{Z^{uP}}) : C(\mathbf{y}) : (\mathbf{Z}^{uE} : \mathbf{E} + \mathbf{Z}^{uP}.\mathbf{E}_{\mathbf{M}}^{\mathbf{elec}}) + (\mathbf{Z^{uE}} : \mathbf{E} + \mathbf{Z^{uP}}.\mathbf{E}_{\mathbf{M}}^{\mathbf{elec}}) : C(\mathbf{y}) : (\mathbf{Z}^{uP}) \\ +(\mathbf{Z^{PP}}).\mathbf{a}.(\mathbf{Z^{PE}} : \mathbf{E} + \mathbf{Z^{PP}}.\mathbf{E}_{\mathbf{M}}^{\mathbf{elec}}) + (\mathbf{Z^{PE}} : \mathbf{E} + \mathbf{Z^{PP}}.\mathbf{E}_{\mathbf{M}}^{\mathbf{elec}}).\mathbf{a}.(\mathbf{Z^{PP}}) \\ +(\mathbf{Z^{uP}}).\mathbf{d}.(\mathbf{Z^{PE}} : \mathbf{E} + \mathbf{Z^{PP}}.\mathbf{E}_{\mathbf{M}}^{\mathbf{elec}}) + (\mathbf{Z^{uE}} : \mathbf{E} + \mathbf{Z^{uP}}.\mathbf{E}_{\mathbf{M}}^{\mathbf{elec}}).\mathbf{d}.(\mathbf{Z^{PP}}) \\ +(\mathbf{Z^{PP}}).\mathbf{d}.(\mathbf{Z^{uE}} : \mathbf{E} + \mathbf{Z^{uP}}.\mathbf{E}_{\mathbf{M}}^{\mathbf{elec}}) + (\mathbf{Z^{PE}} : \mathbf{E} + \mathbf{Z^{PP}}.\mathbf{E}_{\mathbf{M}}^{\mathbf{elec}}).\mathbf{d}.(\mathbf{Z^{uP}}) \end{array} \right\} dV_y$$

$$
\begin{aligned}
&= \frac{1}{2}\left(\int_Y \left\{ \begin{array}{l} \left(\mathbf{Z^{uP}}\right) : C(\mathbf{y}) : \left(\mathbf{Z}^{uE}\right) + \left(\mathbf{Z^{uE}}\right)^T : C(\mathbf{y}) : \left(\mathbf{Z}^{uP}\right) + \left(\mathbf{Z^{PP}}\right).\mathbf{a}.\left(\mathbf{Z^{PE}}\right) + \left(\mathbf{Z^{PE}}\right)^T.\mathbf{a}.\left(\mathbf{Z^{PP}}\right) \\ +\left(\mathbf{Z^{uP}}\right).\mathbf{d}.\left(\mathbf{Z^{PE}}\right) + \left(\mathbf{Z^{uE}}\right)^T.\mathbf{d}.\left(\mathbf{Z^{PP}}\right) + \left(\mathbf{Z^{PP}}\right).\mathbf{d}.\left(\mathbf{Z^{uE}}\right) + \left(\mathbf{Z^{PE}}\right)^T.\mathbf{d}.\left(\mathbf{Z^{uP}}\right) \end{array} \right\} dV_y \right) : \mathbf{E} \\
&+ \frac{1}{2}\left(\int_Y \left\{ \begin{array}{l} \left(\mathbf{Z^{uP}}\right) : C(\mathbf{y}) : \left(\mathbf{Z}^{uP}\right) + \left(\mathbf{Z^{uP}}\right)^T : C(\mathbf{y}) : \left(\mathbf{Z}^{uP}\right) + \left(\mathbf{Z^{PP}}\right).\mathbf{a}.\left(\mathbf{Z^{PP}}\right) + \left(\mathbf{Z^{PP}}\right)^T.\mathbf{a}.\left(\mathbf{Z^{PP}}\right) \\ +\left(\mathbf{Z^{uP}}\right).\mathbf{d}.\left(\mathbf{Z^{PP}}\right) + \left(\mathbf{Z^{uP}}\right)^T.\mathbf{d}.\left(\mathbf{Z^{PP}}\right) + \left(\mathbf{Z^{PP}}\right).\mathbf{d}.\left(\mathbf{Z^{uP}}\right) + \left(\mathbf{Z^{PP}}\right)^T.\mathbf{d}.\left(\mathbf{Z^{uP}}\right) \end{array} \right\} dV_y \right) .\mathbf{E_M^{elec}}
\end{aligned} \quad (A.5)
$$

When extending toward a flexoelectric media, the Lagrangian functional of the displacement and electric potential fluctuations is obtained after substituring the compact localizators in the equation of energy Eq. (24) is as follows:

$$
\begin{aligned}
L\left[\tilde{\mathbf{u}}, \tilde{\phi}\right] &:= \frac{1}{2}\int_Y \left\{\varepsilon : \mathbf{C} : \varepsilon + \mathbf{E_M^{elec}}.\mathbf{a}.\mathbf{E_M^{elec}} + \varepsilon.\mathbf{d}.\mathbf{E_M^{elec}} + \mathbf{E_M^{elec}}.\mathbf{d}.\varepsilon\right\} dV_y \\
&= \frac{1}{2}\int_Y \left\{ \begin{array}{l} \left(\mathbf{Z^{uE}}(\mathbf{y}) : \mathbf{E}(\mathbf{x}) + \mathbf{Z^{uk}}(\mathbf{y}) \therefore \mathbf{K}(\mathbf{x}) + \mathbf{Z^{uP}}(\mathbf{y}).\mathbf{E_M^{elec}}(\mathbf{x}) + \mathbf{Z^{uG_P}}(\mathbf{y}) : \mathbf{G}_p(\mathbf{x})\right) : \mathbf{C}(\mathbf{y}) \\ : \left(\mathbf{Z^{uE}}(\mathbf{y}) : \mathbf{E}(\mathbf{x}) + \mathbf{Z^{uk}}(\mathbf{y}) \therefore \mathbf{K}(\mathbf{x}) + \mathbf{Z^{uP}}(\mathbf{y}).\mathbf{E_M^{elec}}(\mathbf{x}) + \mathbf{Z^{uG_P}}(\mathbf{y}) : \mathbf{G}_p(\mathbf{x})\right) \\ +\left(\mathbf{Z^{PP}}(\mathbf{y}).\mathbf{E_M^{elec}}(\mathbf{x}) + \mathbf{Z^{PE}}(\mathbf{y}).\mathbf{E}(\mathbf{x}) + \mathbf{Z^{PK}}(\mathbf{y}) \therefore \mathbf{K}(\mathbf{x}) + \mathbf{Z^{PG_P}}(\mathbf{y}) : \mathbf{G}_p(\mathbf{x})\right).\mathbf{a}. \\ \left(\mathbf{Z^{PP}}(\mathbf{y}).\mathbf{E_M^{elec}}(\mathbf{x}) + \mathbf{Z^{PE}}(\mathbf{y}).\mathbf{E}(\mathbf{x}) + \mathbf{Z^{PK}}(\mathbf{y}) \therefore \mathbf{K}(\mathbf{x}) + \mathbf{Z^{PG_P}}(\mathbf{y}) : \mathbf{G}_p(\mathbf{x})\right) \\ +\left(\mathbf{Z^{uE}}(\mathbf{y}) : \mathbf{E}(\mathbf{x}) + \mathbf{Z^{uk}}(\mathbf{y}) \therefore \mathbf{K}(\mathbf{x}) + \mathbf{Z^{uP}}(\mathbf{y}).\mathbf{E_M^{elec}}(\mathbf{x}) + \mathbf{Z^{uG_P}}(\mathbf{y}) : \mathbf{G}_p(\mathbf{x})\right).\mathbf{d}. \\ \left(\mathbf{Z^{PP}}(\mathbf{y}).\mathbf{E_M^{elec}}(\mathbf{x}) + \mathbf{Z^{PE}}(\mathbf{y}).\mathbf{E}(\mathbf{x}) + \mathbf{Z^{PK}}(\mathbf{y}) \therefore \mathbf{K}(\mathbf{x}) + \mathbf{Z^{PG_P}}(\mathbf{y}) : \mathbf{G}_p(\mathbf{x})\right) \\ +\left(\mathbf{Z^{PP}}(\mathbf{y}).\mathbf{E_M^{elec}}(\mathbf{x}) + \mathbf{Z^{PE}}(\mathbf{y}).\mathbf{E}(\mathbf{x}) + \mathbf{Z^{PK}}(\mathbf{y}) \therefore \mathbf{K}(\mathbf{x}) + \mathbf{Z^{PG_P}}(\mathbf{y}) : \mathbf{G}_p(\mathbf{x})\right).\mathbf{d}. \\ \left(\mathbf{Z^{uE}}(\mathbf{y}) : \mathbf{E}(\mathbf{x}) + \mathbf{Z^{uk}}(\mathbf{y}) \therefore \mathbf{K}(\mathbf{x}) + \mathbf{Z^{uP}}(\mathbf{y}).\mathbf{E_M^{elec}}(\mathbf{x}) + \mathbf{Z^{uG_P}}(\mathbf{y}) : \mathbf{G}_p(\mathbf{x})\right) \end{array} \right\} dV_y
\end{aligned} \quad (A.6)
$$

The flexoelectric constitutive law is obtained by taking the partial derivatives of the minimum mesoscopic energy in Eq. (24) with respect to **E** and $\mathbf{E_M^{elec}}$, **K**, and $\mathbf{G}_p$ to determine the stress, electric displacement, hyperstress, and higher gradient electric displacement respectively as follows:

$$
\mathbf{\Sigma} = \frac{\partial}{\partial \mathbf{E}}\left(\underset{\tilde{\mathbf{u}},\tilde{\phi}\in H^1_{per}(Y)}{Min} L\left[\tilde{\mathbf{u}}, \tilde{\phi}\right]\right) \equiv \underset{\tilde{\mathbf{u}},\tilde{\phi}\in H^1_{per}(Y)}{Min} \frac{\partial L\left[\tilde{\mathbf{u}}, \tilde{\phi}\right]}{\partial \mathbf{E}} = \frac{1}{2}\int_Y \left\{ \begin{array}{l} 2\left(\mathbf{Z^{uE}} : \mathbf{E} + \mathbf{Z^{uk}} \therefore \mathbf{K} + \mathbf{Z^{uP}}.\mathbf{E_M^{elec}} + \mathbf{Z^{uG_P}} : \mathbf{G}_p\right) : \mathbf{C} : \mathbf{Z^{uE}} \\ +\left(\mathbf{Z^{PE}}\right).\mathbf{a}.\left(\mathbf{Z^{PP}}.\mathbf{E_M^{elec}} + \mathbf{Z^{PE}}.\mathrm{E} + \mathbf{Z^{PK}} \therefore \mathbf{K} + \mathbf{Z^{PGp}} : \mathbf{G}_p\right) \\ +\left(\mathbf{Z^{PP}}.\mathbf{E_M^{elec}} + \mathbf{Z^{PE}}.\mathrm{E} + \mathbf{Z^{PK}} \therefore \mathbf{K} + \mathbf{Z^{PGp}} : \mathbf{G}_p\right).\mathbf{a}.\left(\mathbf{Z^{PE}}\right) \\ +\left(\mathbf{Z^{uE}}\right).\mathbf{d}.\left(\mathbf{Z^{PP}}.\mathbf{E_M^{elec}} + \mathbf{Z^{PE}}.\mathrm{E} + \mathbf{Z^{PK}} \therefore \mathbf{K} + \mathbf{Z^{PGp}} : \mathbf{G}_p\right) \\ +\left(\mathbf{Z^{uE}} : \mathbf{E} + \mathbf{Z^{uk}} \therefore \mathbf{K} + \mathbf{Z^{uP}}.\mathbf{E_M^{elec}} + \mathbf{Z^{uG_P}} : \mathbf{G}_p\right).\mathbf{d}.\left(\mathbf{Z^{PE}}\right) \\ +\left(\mathbf{Z^{PE}}\right).\mathbf{d}.\left(\mathbf{Z^{uE}} : \mathbf{E}(\mathbf{x}) + \mathbf{Z^{uk}} \therefore \mathbf{K} + \mathbf{Z^{uP}}.\mathbf{P} + \mathbf{Z^{uG_P}} : \mathbf{G}_p\right) \\ +\left(\mathbf{Z^{PP}}.\mathbf{E_M^{elec}} + \mathbf{Z^{PE}}.\mathrm{E} + \mathbf{Z^{PK}} \therefore \mathbf{K} + \mathbf{Z^{PGp}} : \mathbf{G}_p\right).\mathbf{d}.\mathbf{Z^{uE}} \end{array} \right\} dV_y \quad (A.7)
$$

By the factorization of Eq. (A.7), the stress tensor expresses versus the kinematic variables as:

$$
\begin{aligned}
\mathbf{\Sigma} &= \left(\frac{1}{2}\int_Y \left\{ \begin{array}{l} 2\left(\mathbf{Z^{uE}}\right)^T : \mathbf{C} : \mathbf{Z^{uE}} + \left(\mathbf{Z^{PE}}\right).\mathbf{a}.\mathbf{Z^{PE}} + \left(\mathbf{Z^{PE}}\right)^T.a.\left(\mathbf{Z^{PE}}\right) + \left(\mathbf{Z}^{uE}\right)^T.\mathbf{d}.\mathbf{Z^{PE}} \\ +\left(\mathbf{Z^{uE}}\right).\mathbf{d}.\mathbf{Z^{PE}} + \left(\mathbf{Z^{PE}}\right).\mathbf{d}.\mathbf{Z^{uE}} + \left(\mathbf{Z^{PE}}\right)^{\mathbf{T}}.\mathbf{d}.\mathbf{Z^{uE}} \end{array} \right\} dV_y \right) : \mathbf{E} \\
&+ \frac{1}{2}\left(\int_Y dV \left\{ \begin{array}{l} 2\left(\mathbf{Z^{uk}}\right)^{\mathbf{T}} : \mathbf{C} : \mathbf{Z^{uE}} + \left(\mathbf{Z^{PE}}\right).\mathbf{a}.\mathbf{Z^{PK}} + \left(\mathbf{Z^{PK}}\right)^T.\mathbf{a}.Z^{PE} \\ +\left(\mathbf{Z}^{uE}\right).\mathbf{d}.\mathbf{Z^{PK}} + \left(\mathbf{Z^{uk}}\right)^{\mathbf{T}}.\mathbf{d}.\left(\mathbf{Z^{PE}}\right) + \left(\mathbf{Z^{PE}}\right).\mathbf{d}.\mathbf{Z^{uk}} + \left(\mathbf{Z^{PK}}\right)^T.\mathbf{d}.\mathbf{Z^{uE}} \end{array} \right\} dV_y \right) \therefore \mathbf{K} \\
&+ \frac{1}{2}\left(\int_Y \left\{ \begin{array}{l} 2\left(\mathbf{Z^{uP}}\right)^T : \mathbf{C} : \mathbf{Z^{uE}} + \left(\mathbf{Z^{PE}}\right).\mathbf{a}.\mathbf{Z^{PP}} + \left(\mathbf{Z^{PP}}\right)^T.\mathbf{a}.\mathbf{Z^{PE}} \\ +\left(\mathbf{Z^{uE}}\right).\mathbf{d}.\mathbf{Z^{PP}} + \left(\mathbf{Z^{uP}}\right)^T.\mathbf{d}.\mathbf{Z^{PE}} + \left(\mathbf{Z^{PE}}\right).\mathbf{d}.\mathbf{Z^{uP}} + \left(\mathbf{Z^{PP}}\right)^T.\mathbf{d}.\mathbf{Z^{uE}} \end{array} \right\} dV_y \right) .\mathbf{E_M^{elec}} \\
&+ \frac{1}{2}\left(\int_Y \left\{ \begin{array}{l} 2\left(\mathbf{Z^{uG}}\right)^T : \mathbf{C} : \mathbf{Z^{uE}} + \left(\mathbf{Z^{PE}}\right).\mathbf{a}.\left(\mathbf{Z^{PGp}}\right) + \left(\mathbf{Z^{PGp}}\right)^T.\mathbf{a}.\mathbf{Z^{PE}} \\ +\left(\mathbf{Z^{uE}}\right).\mathbf{d}.\left(\mathbf{Z^{PGp}}\right) + \left(\mathbf{Z^{uG_P}}\right)^T.\mathbf{d}.\left(\mathbf{Z^{PE}}\right) + \left(\mathbf{Z^{PE}}\right).\mathbf{d}.\left(\mathbf{Z^{uG_P}}\right) + \left(\mathbf{Z^{PGp}}\right)^T.\mathbf{d}.\mathbf{Z^{uE}} \end{array} \right\} dV_y \right) : \mathbf{G}_p
\end{aligned} \quad (A.8)
$$

Similarly, the electric displacement is written as follows:

$$
\begin{aligned}
\overline{\mathbf{D}} &= \frac{\partial}{\partial \mathbf{E_M^{elec}}}\left(\underset{\tilde{\mathbf{u}},\tilde{\phi}\in H^1_{per}(Y)}{Min} L\left[\tilde{\mathbf{u}}, \tilde{\phi}\right]\right) \equiv \underset{\tilde{\mathbf{u}},\tilde{\phi}\in H^1_{per}(Y)}{Min} \frac{\partial L\left[\tilde{\mathbf{u}}, \tilde{\phi}\right]}{\partial \mathbf{E_M^{elec}}} \\
&= \frac{1}{2}\int_Y dV_y \left\{ \begin{array}{l} \left(\mathbf{Z^{uE}}\right)^T : \mathbf{C} : \left(\mathbf{Z^{uP}}\right) + \left(\mathbf{Z^{uP}}\right) : \mathbf{C} : \left(\mathbf{Z^{uE}}\right) + \left(\mathbf{Z^{PP}}\right).\mathbf{a}.\left(\mathbf{Z^{PE}}\right) + \left(\mathbf{Z^{PE}}\right)^T.\mathbf{a}.\left(\mathbf{Z^{PP}}\right) \\ +\left(\mathbf{Z^{uP}}\right).\mathbf{d}.\left(\mathbf{Z^{PE}}\right) + \left(\mathbf{Z^{uE}}\right)^T.\mathbf{d}.\left(\mathbf{Z^{PP}}\right) + \left(\mathbf{Z^{PP}}\right).\mathbf{d}.\left(\mathbf{Z^{uE}}\right) + \left(\mathbf{Z^{PE}}\right)^T.\mathbf{d}.\left(\mathbf{Z^{uP}}\right) \end{array} \right\} : \mathbf{E} \\
&+ \frac{1}{2}\int_Y dV_y \left\{ \begin{array}{l} \left(\mathbf{Z^{uP}}\right) : \mathbf{C} : \mathbf{Z^{uk}} + \left(\mathbf{Z^{uk}}\right)^T : \mathbf{C} : \left(\mathbf{Z^{uP}}\right) + \left(\mathbf{Z^{PP}}\right).\mathbf{a}.\mathbf{Z^{PK}} + \left(\mathbf{Z^{PK}}\right)^T.\mathbf{a}.\mathbf{Z^{PP}} + \\ +\left(\mathbf{Z^{uP}}\right).\mathbf{d}.\mathbf{Z^{PK}} + \left(\mathbf{Z^{uk}}\right)^T.\mathbf{d}.\mathbf{Z^{PP}} + \mathbf{Z^{PP}}.\mathbf{d}.\mathbf{Z^{uk}} + \left(\mathbf{Z^{PK}}\right)^T.\mathbf{d}.\mathbf{Z^{uP}} \end{array} \right\} \therefore \mathbf{K}
\end{aligned}
$$

$$+\frac{1}{2}\left(\int_Y dV_y\left\{\begin{array}{l}(\mathbf{Z^{uP}}):\mathbf{C}:\mathbf{Z^{uP}}+(\mathbf{Z^{uP}})^T:\mathbf{C}:\mathbf{Z^{uP}}+\mathbf{Z^{PP}}.\mathbf{a}.\mathbf{Z^{PP}}+(\mathbf{Z^{PP}})^T.\mathbf{a}.\mathbf{Z^{PP}}+\mathbf{Z^{uP}}.\mathbf{d}.\mathbf{Z^{PP}}\\+(\mathbf{Z^{uP}})^T.\mathbf{d}.\mathbf{Z^{PP}}+\mathbf{Z^{PP}}.\mathbf{d}.\mathbf{Z^{uP}}+(\mathbf{Z^{PP}})^T.\mathbf{d}.\mathbf{Z^{uP}}\end{array}\right\}\right).\mathbf{E^{elec}_M}$$
$$+\frac{1}{2}\left(dV_y\int_Y\left\{\begin{array}{l}(\mathbf{Z^{uP}}):\mathbf{C}:\mathbf{Z^{uG_P}}+(\mathbf{Z^{uG_P}})^T:\mathbf{C}(\mathbf{y}):\mathbf{Z^{uP}}+\mathbf{Z^{PP}}.\mathbf{a}.\mathbf{Z^{PGp}}+(\mathbf{Z^{PGp}})^T.\mathbf{a}.\mathbf{Z^{PP}}\\+(\mathbf{Z^{uP}}).\mathbf{d}.\mathbf{Z^{PGp}}+(\mathbf{Z^{uG_P}})^T.\mathbf{d}.\mathbf{Z^{PP}}+\mathbf{Z^{PP}}.\mathbf{d}.\mathbf{Z^{uG_P}}+(\mathbf{Z^{PGp}})^T.\mathbf{d}.\mathbf{Z^{uP}}\end{array}\right\}\right):\mathbf{G}_p \tag{A.9}$$

As to higher gradient effects, the hyperstress is derived as follows:

$$\mathbf{S}:=\frac{\partial}{\partial\mathbf{K}}\left(\underset{\tilde{\mathbf{u}},\tilde{\phi}\in H^1_{per}(Y)}{Min}L[\tilde{\mathbf{u}},\tilde{\phi}]\right)\equiv\underset{\tilde{\mathbf{u}},\tilde{\phi}\in H^1_{per}(Y)}{Min}\frac{\partial L[\tilde{\mathbf{u}},\tilde{\phi}]}{\partial\mathbf{K}}$$
$$=\frac{1}{2}\int_Y dV_y\left\{\begin{array}{l}(\mathbf{Z^{uk}}):\mathbf{C}:\mathbf{Z^{uE}}+(\mathbf{Z^{uE}})^T:\mathbf{C}:\mathbf{Z^{uk}}+\mathbf{Z^{PK}}.\mathbf{a}.\mathbf{Z^{PE}}+(\mathbf{Z^{PE}})^T.\mathbf{a}.\mathbf{Z^{PK}}\\+(\mathbf{Z^{uk}}).\mathbf{d}.\mathbf{Z^{PE}}+(\mathbf{Z^{uE}})^T.\mathbf{d}.\mathbf{Z^{PK}}+(\mathbf{Z^{PK}}).\mathbf{d}.\mathbf{Z}^{uE}+(\mathbf{Z^{PE}})^T.\mathbf{d}.\mathbf{Z^{uk}}\end{array}\right\}:\mathbf{E}$$
$$\frac{1}{2}\left(\int_Y dV_y\left\{\begin{array}{l}(\mathbf{Z^{uk}}):\mathbf{C}:\mathbf{Z^{uk}}+(\mathbf{Z^{uk}})^T:\mathbf{C}:\mathbf{Z^{uk}}+\mathbf{Z^{PK}}.\mathbf{a}.\mathbf{Z^{PK}}+(\mathbf{Z^{PK}})^T.\mathbf{a}.\mathbf{Z^{PK}}\\+\mathbf{Z^{uk}}.\mathbf{d}.(\mathbf{Z^{PK}})+(\mathbf{Z^{uk}})^T.\mathbf{d}.\mathbf{Z^{PK}}+\mathbf{Z^{PK}}.\mathbf{d}.(\mathbf{Z^{uk}})+(\mathbf{Z^{PK}})^T.\mathbf{d}.\mathbf{Z^{uk}}\end{array}\right\}\right)\therefore\mathbf{K}$$
$$\frac{1}{2}\left(\int_Y dV_y\left\{\begin{array}{l}(\mathbf{Z^{uk}}):\mathbf{C}:\mathbf{Z^{uP}}+(\mathbf{Z^{uP}})^T:\mathbf{C}:\mathbf{Z^{uk}}+\mathbf{Z^{PK}}.\mathbf{a}.\mathbf{Z^{PP}}+(\mathbf{Z^{PP}})^T.\mathbf{a}.\mathbf{Z^{PK}}\\+\mathbf{Z^{uk}}.\mathbf{d}.\mathbf{Z^{PP}}+(\mathbf{Z^{uP}})^T.\mathbf{d}.\mathbf{Z^{PK}}+\mathbf{Z^{PK}}.\mathbf{d}.\mathbf{Z^{uP}}+(\mathbf{Z^{PP}})^T.\mathbf{d}.\mathbf{Z^{uk}}\end{array}\right\}\right).\mathbf{E^{elec}_M}$$
$$\frac{1}{2}\left(\int_Y dV_y\left\{\begin{array}{l}(\mathbf{Z^{uk}}):\mathbf{C}:\mathbf{Z^{uG}}+(\mathbf{Z^{uG}})^T:\mathbf{C}:\mathbf{Z^{uk}}+\mathbf{Z^{PK}}.\mathbf{a}.\mathbf{Z^{PGp}}+(\mathbf{Z^{PGp}})^T.\mathbf{a}.\mathbf{Z^{PK}}\\+\mathbf{Z^{uk}}.\mathbf{d}.\mathbf{Z^{PGp}}+(\mathbf{Z^{uG}})^T.\mathbf{d}.\mathbf{Z^{PK}}+\mathbf{Z^{PK}}.\mathbf{d}.\mathbf{Z^{uG}}+(\mathbf{Z^{PGp}})^T.\mathbf{d}.\mathbf{Z^{uk}}\end{array}\right\}\right):\mathbf{G}_p \tag{A.10}$$

Also, the higher gradient electric displacement second order tensor can be obtained as follows:

$$\mathbf{R}:=\frac{\partial}{\partial\mathbf{G}_p}\left(\underset{\tilde{\mathbf{u}},\tilde{\phi}\in H^1_{per}(Y)}{Min}L[\tilde{\mathbf{u}},\tilde{\phi}]\right)\equiv\underset{\tilde{\mathbf{u}},\tilde{\phi}\in H^1_{per}(Y)}{Min}\frac{\partial L[\tilde{\mathbf{u}},\tilde{\phi}]}{\partial\mathbf{G}_p}$$
$$=\frac{1}{2}\left(\int_Y dV_y\left\{\begin{array}{l}(\mathbf{Z^{uG_P}}):\mathbf{C}:\mathbf{Z^{uE}}+(\mathbf{Z^{uE}})^T:\mathbf{C}:\mathbf{Z^{uG_P}}+\mathbf{Z^{PGp}}.\mathbf{a}.\mathbf{Z^{PE}}+(\mathbf{Z^{PE}})^T.\mathbf{a}.\mathbf{Z^{PGp}}\\+\mathbf{Z^{uG_P}}.\mathbf{d}.\mathbf{Z^{PE}}+(\mathbf{Z^{uE}})^T.\mathbf{d}.\mathbf{Z^{PGp}}+\mathbf{Z^{PGp}}.\mathbf{d}.\mathbf{Z^{uE}}+(\mathbf{Z^{PE}})^T.\mathbf{d}.\mathbf{Z^{uG_P}}\end{array}\right\}\right):\mathrm{E}$$
$$+\frac{1}{2}\left(\int_Y dV_y\left\{\begin{array}{l}\mathbf{Z^{uG_P}}:\mathbf{C}:\mathbf{Z^{uk}}+(\mathbf{Z^{uk}})^T:\mathbf{C}:\mathbf{Z^{uG_P}}+\mathbf{Z^{PGp}}.\mathbf{a}.\mathbf{Z^{PK}}+(\mathbf{Z^{PK}})^T.\mathbf{a}.\mathbf{Z^{PGp}}+\\+\mathbf{Z^{uG_P}}.\mathbf{d}.\mathbf{Z^{PK}}+(\mathbf{Z^{uk}})^T.\mathbf{d}.\mathbf{Z^{PGp}}+\mathbf{Z^{PGp}}.\mathbf{d}.\mathbf{Z^{uk}}+(\mathbf{Z^{PK}})^T.\mathbf{d}.\mathbf{Z^{uG_P}}\end{array}\right\}\right)\therefore\mathbf{K}$$
$$+\frac{1}{2}\left(\int_Y dV_y\left\{\begin{array}{l}\mathbf{Z^{uG_P}}:\mathbf{C}:\mathbf{Z^{uP}}+(\mathbf{Z^{uP}})^T:\mathbf{C}:\mathbf{Z^{uG_P}}+\mathbf{Z^{PGp}}.\mathbf{a}.\mathbf{Z^{PP}}+(\mathbf{Z^{PP}})^T.\mathbf{a}.\mathbf{Z^{PGp}}\\+\mathbf{Z^{uG_P}}.\mathbf{d}.\mathbf{Z^{PP}}+(\mathbf{Z^{uP}})^T.\mathbf{d}.\mathbf{Z^{PGp}}+\mathbf{Z^{PGp}}.\mathbf{d}.\mathbf{Z^{uP}}+(\mathbf{Z^{PP}})^T.\mathbf{d}.\mathbf{Z^{uG_P}}\end{array}\right\}\right).\mathbf{E^{elec}_M}$$
$$+\frac{1}{2}\left(\int_Y dV_y\left\{\begin{array}{l}\mathbf{Z^{uG_P}}:\mathbf{C}:\mathbf{Z^{uG}}+(\mathbf{Z^{uG}})^T:\mathbf{C}:\mathbf{Z^{uG_P}}+\mathbf{Z^{PGp}}.\mathbf{a}.\mathbf{Z^{PGp}}+(\mathbf{Z^{PGp}})^T.\mathbf{a}.\mathbf{Z^{PGp}}\\+\mathbf{Z^{uG_P}}.\mathbf{d}.\mathbf{Z^{PGp}}+(\mathbf{Z^{uG}})^T.\mathbf{d}.\mathbf{Z^{PGp}}+\mathbf{Z^{PGp}}.\mathbf{d}.\mathbf{Z^{uG}}+(\mathbf{Z^{PGp}})^T.\mathbf{d}.\mathbf{Z^{uG_P}}\end{array}\right\}\right):\mathbf{G}_p \tag{A.11}$$

Appendix B

A comparison between the results obtained in our variational approach and the analytical model in Sevostianov and Sabina (2007) was made. The materials used were BaTiO3 for the fiber and PZT-5H for the matrix with their properties presented in Table 2.

Figs. (B.1)-(B.2)-(B.3) show a good agreement between the results obtained using the variational approach and the results in Sevostianov and Sabina (2007) for the dielectric and piezoelectric coefficients with a maximum relative error for the piezoelectric coefficients (d_{31} and d_{33}) 3%, and for the dielectric coefficient (permittivity) around 1%.

Table 2
Mechanical and electrical properties of the two piezoelectric materials within the unit cell of the composite material.

	C_{11}(GPa)	C_{33}(GPa)	C_{12}(GPa)	C_{13}(GPa)	d_{31}(C/m^2)	d_{33}(C/m^2)	a_{11}(nF/m)	a_{33}(nF/M)
BaTiO3	166	162	77	78	-4.4	18.6	11.2	12.6
PZT-5H	126	117	55	53	-6.5	23.3	15.1	13

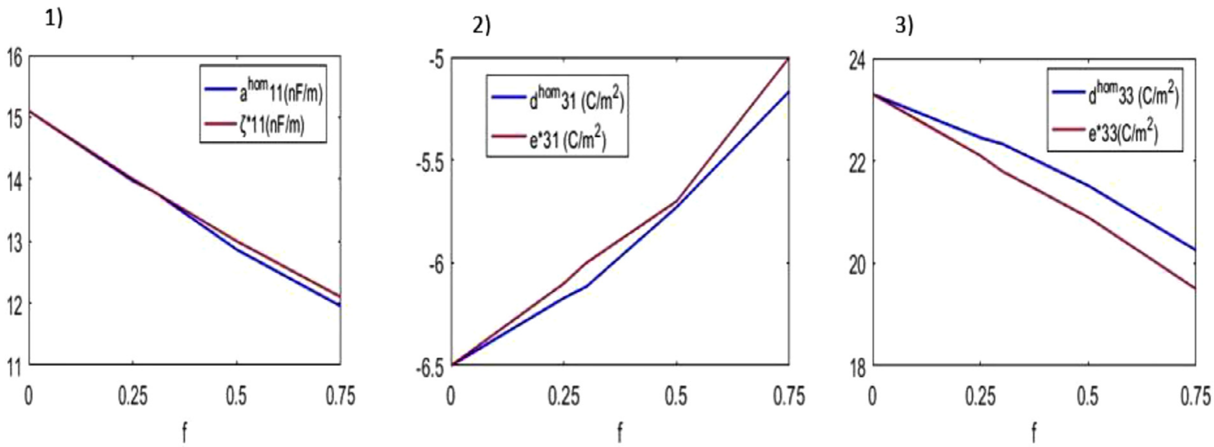

Fig. B. Variation of the 1) dielectric coefficient, 2) and 3) piezoelectric coefficients as a function of the volume fraction. 'Red color' 'blue color' corresponds to the results in (Sevostianov & Sabina, 2007), blue corresponds to the results using the variational approach.

References

Abdoul-Anziz, H., & Seppecher, P. (2018). Strain gradient and generalized continua obtained by homogenizing frame lattices. *Mathematics and Mechanics of Complex Systems, 6*(3), 213–250.

Barati, M. R. (2017). On non-linear vibrations of flexoelectric nanobeams. *International Journal of Engineering Science, 121*, 143–153.

Buechner, P. M., & Lakes, R. S. (2003). Size effects in the elasticity and viscoelasticity of bone. *Biomechanics and Modeling in Mechanobiology, 1*(4), 295–301.

Casalotti, A., D'Annibale, F., & Rosi, G. (2020). Multi-scale design of an architected composite structure with optimized graded properties. *Composite Structures, 252*, Article 112608.

Chambion, B., Goujon, L., Badie, L., Mugnier, Y., Barthod, C., Galez, C., Wiebel, S., & Venet, C. (2011). Optimization of the piezoelectric response of 0–3 composites: a modeling approach. *Smart materials and Structures, 20*(11), Article 115006.

Cioranescu, D., & Donato, P. (1999). *An introduction to homogenization*: 17. Oxford: Oxford University Press.

Cosserat, E., & Cosserat, F. (1896). Sur la théorie de l'elasticité. *Ann Toulouse, 10*, 1–116.

Cosserat, E., & Cosserat, F. (1909). *Théorie des corps déformables*. Paris: Herman et Fils.

Deng, Q., Kammoun, M., Erturk, A., & Sharma, P. (2014). Nanoscale flexoelectric energy harvesting. *International Journal of Solids and Structures, 51*(18), 3218–3225.

Eremeyev, V. A., Ganghoffer, J.-F., Konopińska-Zmys lowska, V., & Uglov, N. S. (2020). Flexoelectricity and apparent piezoelectricity of a pantographic micro-bar. *International Journal of Engineering Science, 149*, Article 103213.

Eringen, A. C. (1999). *Microcontinuum field theory. I. Foundations and solids*. New York: Springer.

Eringen, A. C., & Maugin, G. A. (1990). *Electrodynamics of continua*. New York: Springer.

Ghayesh, M. H., & Farajpour, A. (2019). A review on the mechanics of functionally graded nanoscale and microscale structures. *International Journal of Engineering Science, 137*, 8–36.

Grekov, A. A., Kramarov, S. O., & Kuprienko, A. A. (1987). Anomalous behavior of the two-phase lamellar piezoelectric texture. *Ferroelectrics, 76*(1), 43–48.

Guinovart-Sanjuán, D., Merodio, J., López-Realpozo, J. C., Vajravelu, K., Rodr´ıguez-Ramos, R., Guinovart-D´ıaz, R., Bravo-Castillero, J., & Sabina, F. J. (2019). Asymptotic homogenization applied to flexoelectric rods. *Materials, 12*(2), 232.

Hill, R. (1967). The essential structure of constitutive laws for metal composites and polycrystals. *Journal of the Mechanics and Physics of Solids, 15*(2), 79–95.

Hong, J. (2018). Beyond piezoelectricity: Flexoelectricity in solids. *Journal Club for November.*, 4.

Kogan, S. M. (1964). Piezoelectric effect during inhomogeneous deformation and acoustic scattering of carriers in crystals. *Soviet Physics — Solid State, 5*(10), 2069–2070.

Le Quang, H., & He, Q.-C. (2011). The number and types of all possible rotational symmetries for flexoelectric tensors. In *Proceedings of the royal society a: mathematical, physical and engineering sciences: 467* (pp. 2369–2386).

Liang, X., Zhang, R., Hu, S., & Shen, S. (2017). Flexoelectric energy harvesters based on Timoshenko laminated beam theory. *Journal of Intelligent Material Systems and Structures, 28*(15), 2064–2073.

Liu, C., Wu, H., & Wang, J. (2016). Giant piezoelectric response in piezoelectric/dielectric superlattices due to flexoelectric effect. *Applied Physics Letters, 109*(19), Article 192901.

Majdoub, M. S., Sharma, P., & Cagin, T. (2008). Enhanced size-dependent piezoelectricity and elasticity in nanostructures due to the flexoelectric effect. *Physical Review B, 77*(12), Article 125424.

Malikan, M., & Eremeyev, V. A. (2020). On the geometrically nonlinear vibration of a piezo-flexomagnetic nanotube. *Mathematical Methods in the Applied Sciences*. https://doi.org/10.1002/mma.6758.

Maugin, G. A. (1988). *Continuum mechanics of electromagnetic solids*. Oxford: Elsevier.

Meyer, R. B. (1969). Piezoelectric effects in liquid crystals. *Physical Review Letters, 22*(18), 918–921.

Mindlin, R. D. (1964). Micro-structure in linear elasticity. *Archive for Rational Mechanics and Analysis, 16*(1), 51–78.

Mindlin, R. D. (1968). Polarization gradient in elastic dielectrics. *International Journal of Solids and Structures, 4*(6), 637–642.

Nanthakumar, S. S., Zhuang, X., Park, H. S., & Rabczuk, T. (2017). Topology optimization of flexoelectric structures. *Journal of the Mechanics and Physics of Solids, 105*, 217–234.

Nguyen, T. D., Mao, S., Yeh, Y.-W., Purohit, P. K., & McAlpine, M. C. (2013). Nanoscale flexoelectricity. *Advanced Materials, 25*(7), 946–974.

Park, H. C., & Lakes, R. S. (1986). Cosserat micromechanics of human bone: strain redistribution by a hydration-sensitive constituent. *Journal of Biomechanics, 19*(5), 385–397.

Qi, L., Huang, S., Fu, G., Zhou, S., & Jiang, X. (2018). On the mechanics of curved flexoelectric microbeams. *International Journal of Engineering Science, 124*, 1–15.

Rahali, Y., Dos Reis, F., & Ganghoffer, J.-F. (2017). Multiscale homogenization schemes for the construction of second-order grade anisotropic continuum media of architectured materials. *International Journal for Multiscale Computational Engineering, 15*(1), 1–44.

Reda, H., Karathanasopoulos, N., Maurice, G., Ganghoffer, J. F., & Lakiss, H. (2020). Computation of effective piezoelectric properties of stratified composites and application to wave propagation analysis. *ZAMM, 100*(2), Article e201900251.

Sevostianov, I., Levin, V., & Kachanov, M. (2001). On the modeling and design of piezocomposites with prescribed properties. *Archive of Applied Mechanics, 71*(11), 733–747.

Sevostianov, I., & Sabina, F. J. (2007). Cross-property connections for fiber reinforced piezoelectric materials with anisotropic constituents. *International Journal of Engineering Science, 45*(9), 719–735.

Sharma, N. D., Maranganti, R., & Sharma, P. (2007). On the possibility of piezoelectric nanocomposites without using piezoelectric materials. *Journal of the Mechanics and Physics of Solids, 55*(11), 2328–2350.

Shingare, K. B., & Kundalwal, S. I. (2019). Static and dynamic response of graphene nanocomposite plates with flexoelectric effect. *Mechanics of Materials, 134*, 69–84.

Tartar, L. (1990). H-measures, a new approach for studying homogenisation, oscillations and concentration effects in partial differential equations. In *Proceedings of the Royal Society of Edinburgh Section A: Mathematics: 115* (pp. 193–230).

Toupin, R. A. (1962). Elastic materials with couple-stresses. *Archive for Rational Mechanics and Analysis, 11*(1), 385–414.

Wang, B., Gu, Y., Zhang, S., & Chen, L.-Q. (2019). Flexoelectricity in solids: progress, challenges, and perspectives. *Progress in Materials Science, 106*, Article 100570.

Yang, J. (2006). *Analysis of piezoelectric devices*. New Jersey: World Scientific.

Yudin, P. V., & Tagantsev, A. K. (2013). Fundamentals of flexoelectricity in solids. *Nanotechnology, 24*(43), Article 432001.

Yue, Y. M., Xu, K. Y., & Chen, T. (2016). A micro scale Timoshenko beam model for piezoelectricity with flexoelectricity and surface effects. *Composite Structures, 136*, 278–286.

Zhang, S., Xu, M., Liu, K., & Shen, S. (2015). A flexoelectricity effect-based sensor for direct torque measurement. *Journal of Physics D: Applied Physics, 48*(48), Article 485502.

Zubko, P., Catalan, G., & Tagantsev, A. K. (2013). Flexoelectric effect in solids. *Annual Review of Materials Research, 43*(1), 387–421.